ELSEVIER

The nature of coarse-grained crystalline hematite and its implications for the early environment of Mars

David C. Catling [a,*] and Jeffrey M. Moore [b]

[a] Astrobiology Program and Department of Atmospheric Sciences, University of Washington, Box 351640, Seattle, WA 98195-1640, USA
[b] MS 245-3, Space Science Division, NASA Ames Research Center, Moffett Field, CA 93035-1000, USA

Abstract

The Thermal Emission Spectrometer (TES) on the Mars Global Surveyor spacecraft has detected deposits of coarse-grained, gray crystalline hematite in Sinus Meridiani, Aram Chaos, and Vallis Marineris. We argue that the key to the origin of gray hematite is that it requires crystallization at temperatures in excess of about 100 °C. We discuss thermal crystallization (1) as diagenesis at a depth of a few kilometers of sediments originally formed in low-temperature waters, or (2) as precipitation from hydrothermal solution. In Aram Chaos, a combination of TES data, Mars Orbiter Camera images, and Mars Orbiter Laser Altimeter (MOLA) topography suggests that high concentrations of hematite were formed in planar strata and have since been exposed by erosion of an overlying light-toned, caprock. Lesser concentrations of hematite are found adjacent to these strata at lower elevations, which we interpret as perhaps due to accumulation from physical weathering. The topography and the collapsed nature of the chaotic terrain favor a hydrothermally charged aquifer as the original setting where the hematite formed. Concentration of iron into such an ore-like body would be chemically favored by saline, Cl-rich hydrothermal fluids. An alternative sedimentary origin requires post-depositional burial to a depth of $\sim$ 3–5 km to induce thermally driven recrystallization of fine-grained iron oxides to coarse-grained hematite. This depth of burial and re-exposure is difficult to reconcile with commonly inferred martian geological processes. However, shallow burial accompanied by post-burial hydrothermal activity remains plausible. When the hematite regions originally formed, redox balance requires that much hydrogen must have been evolved to complement the extensive oxidation. Finally, we suggest that the coexistence of several factors required to form the gray hematite deposits would have produced a favorable environment for primitive life on early Mars, if it ever existed. These factors include liquid water, abundant electron donors in the form of H_2, and abundant electron acceptors in the form of Fe^{3+}.

1. Introduction

Iron-rich minerals are important on Mars. Iron comprises about one fifth of the weight of the soil and 16 ± 1 wt% average abundance in rocks observed at the Mars Pathfinder site (Wänke et al., 2001). Generally speaking, the ferrous (Fe^{2+}) and ferric (Fe^{3+}) oxidation states of iron reflect unweathered and weathered components of the martian surface, respectively (Banin et al., 1992). The global surface mineralogy on Mars can be grouped into these two gross compositions:

(1) dark areas spectrally distinguished by Fe^{2+} infrared absorption bands that are pristine mafic or perhaps ul-

tramafic composition on the basis of inferences from spectroscopy and other geochemical data for Mars (e.g., Baird and Clark, 1981; Reyes and Christensen, 1993; Bouska and Bell, 1993; McSween, 1994), and

(2) light areas distinguished by Fe^{3+} (e.g., Morris et al., 1989, 2000).

There are possible exceptions to this rule, however: Fe^{2+} could occur in secondary minerals such as hydrous iron silicates, siderite ($FeCO_3$) or certain clays that would tend to form under reducing conditions perhaps generally characteristic of primordial Mars (Calvin, 1998; Catling, 1999; Wyatt and McSween, 2002). Mars' reddish surface (e.g., Morris et al., 1997, 2000) and the butterscotch color of the martian sky (Huck et al., 1977) are both due to the optical properties of ferric iron oxides (hematite, goethite, or

* Corresponding author.
 E-mail address: davidc@atmos.washington.edu (D.C. Catling).

maghemite) in finely crystalline or poorly crystalline form on the surface and in airborne dust. The existence of local surface concentrations of another ferric component, coarse-grained crystalline hematite, has been established by the Thermal Emission Spectrometer (TES) on Mars Global Surveyor (MGS) (Christensen et al., 2000, 2001). Unlike fine-grained hematite (Morris et al., 1985), coarsely crystalline hematite with grain size > 5 μm is colored gray and has distinctive absorption bands at visible and near-infrared wavelengths (Sherman and Waite, 1985) that are absent from the spectra of ferric-bearing bright regions on Mars (Lane et al., 2002b). Significant deposits of such gray hematite are spectrally inferred to exist in Sinus Meridiani, Aram Chaos, and Vallis Marineris (Christensen et al., 2000, 2001), where they cover areas of > 175,000 km^2, ~ 5000 km^2, and 25–800 km^2, respectively. These deposits are intriguing because of their relatively localized extent and association with geomorphology that appears layered and sedimentary (Christensen et al., 2000, 2001). The Sinus Meridiani deposit may also have an ancient age > 4 Ga based on saturated counts of exhumed "fossil" craters—craters that were once buried and embedded in the subsurface (Kelsey et al., 2000; Hartmann et al., 2001). However, some also argue that the fossil crater count suggests a late Noachian or early Hesperian age (Gilmore and Tanake, 2002). Geomorphology arguments have also been presented to support contrasting views about the southern boundary contact of the Sinus Meridiani hematite with ancient highland terrain. The hematite may mantle the underlying ancient surface (Hynek and Phillips, 2001; Hynek et al., 2002) or the hematite could be an exposure of the underlying ancient bedrock (Malin and Edgett, 2001). Detailed features in the hematite TES spectral signature of the Sinus Meridiani region show that the spectrum is consistent with emission dominated by crystal c-faces of hematite (Lane et al., 2000, 2001, 2002a, 2002b). This has led Lane et al. to suggest that the hematite is dominated by platy grains and that low-grade metamorphism may be required to make such plates when the hematite crystallized (Lane et al., 2002b). Such martian hematite may preserve weak magnetic remanence. Above the so-called Morin transition temperature, $T_M = -10\,°C$, crystalline hematite possesses a weak spin-canted magnetic moment with electron spins in the c-planes (perpendicular to the axis of symmetry), while below T_M hematite is perfectly antiferromagnetic with electron spins precisely antiparallel-aligned along the c-axis so that the only magnetism is that due to defects (Parkinson, 1983, p. 145); however, for reasons that are currently unknown, heating hematite above T_M can make it "remember" a previous field (De Boer et al., 2001). Sinus Meridiani is the largest hematite region (Christensen et al., 2001) and is the landing site of one of NASA's Mars Exploration Rovers (MERs), called MER-B or "Opportunity," launched in July, 2003 (Golombek et al., 2002). Indeed, as we suggest in this paper, the origin of the crystalline hematite may hold significant chemical clues to the early martian environment.

The purpose of this paper is to consider constraints on the origin of the deposits of martian gray hematite, both chemical and physical, and then to reflect on possible broader environmental implications for early Mars. In the first part of the paper, we consider chemical mechanisms to make gray hematite. Christensen et al. (2000, 2001) favor aqueous deposition for the original hematite. An alternative suggestion is that the hematite may be derived from ignimbrites, that is to say compacted, volcanic ash that somehow was oxidized (Tanaka et al., 2000; Noreen et al., 2001). However, the likely grain size of the basaltic host rock in Sinus Meridiani makes air-fall unlikely (Christensen et al., 2001). We review the chemical formation of gray crystalline hematite on Earth. By examining the physical conditions under which gray hematite forms on Earth and the relevant geochemical thermodynamics, we deduce that martian hematite must have crystallized in a warm environment in excess of roughly 100 °C.

In the second part of the paper, we focus on the geology of the Aram Chaos deposit. We specially consider Aram Chaos because its unique topographic relief and chaotic terrain perhaps offer more clues to the formation of the hematite than the more featureless flat terrain (as seen from orbit) of Sinus Meridiani. We examine Mars Orbiter Laser Altimeter (MOLA) data and Mars Orbiter Camera (MOC) images within the hematite-rich region identified by TES spectral mapping to help constrain the geologic context in which the Aram Chaos hematite formed.

Finally, we consider the redox environment on early Mars. In the absence of life, the formation of the hematite must have required water as an oxidant, that is, as the ultimate source of O in Fe$_2$O$_3$. Hematite is commonly the most oxidized form of iron, although unusual higher oxidation states have been proposed for martian surface materials (Tsapin et al. 2000, 2002; Levin, 2002). In any case, deposits of ferric oxides occurring at very early times in martian history are important from a redox perspective. Proponents of both an aqueous origin (Christensen et al., 2000) and an igneous origin (Noreen et al., 2001) have implied that highly oxidizing conditions are needed. The source of oxygen in Fe$_2$O$_3$ is an interesting issue given that early Mars was continuously volcanically active (e.g., Greeley, 1987; Schubert et al., 2001, pp. 691–698). As we show below, the chemistry of the martian paleoatmosphere would be expected to reflect the presence of weakly reducing volcanic gases, which would consume photochemically produced oxygen, giving an equilibrium level of O$_2$ many orders of magnitude less than in the present martian atmosphere. If the hematite deposits are truly ancient (~ 4 Ga), their formation in a weakly reducing environment requires an explanation for how such concentrated oxidation occurred on such a large scale. We deduce that the only abiotic possibility is that ferrous iron was oxidized by thermally dissociated water, with the emanation of hydrogen. This can only be accomplished in a hydrothermal environment rather than a low temperature setting. Finally, we will argue that the presence

of abundant electron acceptors in the form of Fe^{3+} and abundant electron donors in the form H_2 would have provided a redox environment that should have been very favorable for simple Earth-like life on Mars if it ever arose.

2. What are gray hematite and specular hematite?

Before discussing how gray crystalline hematite forms, it is important to define our terms and describe the nature of hematite more precisely. Particle size influences the color of hematite because the reflectance in the red part of the spectrum decreases as particle size (or the size of particle aggregates) gets larger (e.g., Lane et al., 1999). Particles with sizes 1.5–5 µm, 0.1–0.5 µm, and < 0.1 µm grade from purple to red to orange, respectively (Kerker et al., 1979). Grain shape also has an influence, with needles tending to be yellower than cube-like particles (Hund, 1981). In coarsely crystalline form, with > 5 µm crystal size, hematite is gray with a reflectivity typically ∼ 0.1–0.3, sometimes so dark as to appear black. Gray specular hematite (known as "specularite") is a gray crystalline form that has intergrown, hexagonal plates with a silvery metallic luster. The term "specular," of course, means that when light hits the mineral surface the angle of incidence is equal to the angle of reflection. The faces of large, natural crystals thus often have a mirror-like appearance. It is intuitively obvious that the formation process for coarsely crystalline hematite is bound to be quite different from the familiar (terrestrial) oxidative weathering process that ubiquitously forms familiar red-colored, fine-grained hematite. We describe below how coarsely crystalline gray hematite only occurs on Earth as a result of thermal processing.

3. How does gray hematite form on Earth?

The mechanisms for forming gray, crystalline hematite on Earth obviously provide clues to its formation on Mars. Consequently, we review the terrestrial occurrence of gray hematite extensively. On Earth, crystalline hematite deposits form as a result of igneous, sedimentary or hydrothermal processes. We review these formation mechanisms in turn, considering their applicability to Mars.

3.1. Hematite formation in "igneous" environments

The occurrence of crystalline hematite on Mars has naturally led some to favor an association with an igneous origin such as volcanic ash or even direct ascent from volcanism motivated by the observation that Mars is overwhelmingly dominated by volcanic rocks (Tanaka et al., 2000). As we discuss below, hematite arises only as an alteration product of igneous rock and special alteration conditions are required for forming gray, crystalline hematite.

3.1.1. Why hematite lavas do not exist

There is no such thing as "hematite lava" because the oxygen fugacity (f_{O_2}) of magmas is too low to support hematite thermodynamically. A typical oxygen fugacity (f_{O_2}) in terrestrial magma is ∼ 10^{-8} bar at a magmatic temperature (1200 °C) and pressure (5 kbar) (Holland, 1984, p. 49) for which it is not possible for hematite to be a mineral phase in the melt, so hematite does not directly ascend from volcanoes. Hematite is not a possible phase because the f_{O_2} value is about four orders of magnitude lower than the magnetite–hematite buffer and instead close to the synthetic fayalite–magnetite–quartz (FMQ) buffer (e.g., Frost, 1991; Delano, 2001). Estimates for magmatic f_{O_2} on Mars are similar to those on Earth or lower. They range from about FMQ to four log units below FMQ based on studies of redox-sensitive geochemical indicators in martian meteorites (Herd and Papike, 2000; Wadhwa, 2001). Thus the direct ascent of a hematite lava should be even more improbable on Mars than Earth. Furthermore, a hematite lava, were such a thing to exist, would be extremely dense, perhaps irreconcilable with the 10^5 km^2 aerial extent of the Sinus Meridiani deposit and the lack of lava flow features. Direct volcanic ascent of crystalline hematite on Mars has been suggested based on a hypothesized association with andesite and higher water contents and oxygen fugacities in relation to basalts (Chapman and Tanake, 2002). However, such direct ascent is doubtful for several reasons. First, according to Christensen et al., 2001 the dominant host rock in the martian hematite locations is basalt and not andesite. Second, the oxygen fugacity for terrestrial andesites is buffered by ferrous iron and in oxidized cases is only about $2 \log_{10}$ units higher than FMQ (Wood, 1991; Blatter and Carmichael, 1998), which is still two orders of magnitude too low to be able to give rise to a hematite lava. Third, it is not the presence of water that leads to the higher oxygen fugacity in terrestrial andesitic lavas but more likely ferric iron that derives from subducted crust and ferric iron-rich sediment melt (Frost and Ballhaus, 1998; Parkinson and Arculus, 1999), which have no obvious analogues on Mars. Finally, as discussed below, the occurrence of specular hematite in association with andesite in some terrestrial occurrences is most likely a result of hydrothermal activity and post-depositional alteration. Thus, the direct ascent of a hematite lava is improbable given that magmatic oxygen fugacity on Mars is unlikely to ever lie in the hematite stability field.

3.1.2. Hematite from oxidation of igneous rocks

When hematite is found in direct association with terrestrial igneous rocks it is usually as a late-stage product due to oxidation in Earth's oxidizing, O_2-rich surface environment or due to hydrothermal oxidation. Indeed, iron-rich basaltic lavas extruded onto Earth's O_2-rich surface environment are often red because of the presence of finely divided hematite (Best, 1982, p. 286). Hematite is also found in igneous rocks poor in ferrous iron, such as in rhyolites, where the small

amount of iron can be rapidly oxidized in Earth's O_2-rich atmosphere. However, neither such a highly acid rock nor often the type of hematite formed is a suitable analog for the martian deposits. For example, rhyolite is usually red or pink, indicating fine-grained iron oxide (Williams et al., 1954, Chapter 7; Best, 1982, p. 91). Nonetheless, in the Pilot Knob hematite deposit in the St. Francois Mountains of Missouri, steel-gray specular hematite is present in an ore body where the surrounding volcanic rocks are rhyolitic. Here, the origin of the hematite ore is widely held to be hydrothermal, given the occurrence of hematite veins (some as much as 3 m in width) and radiating veinlets, cavity fills, and mineral features like tourmaline that are indicative of warm temperatures (Seeger et al., 1989). Another hydrothermal example of oxidation of rhyolitic rocks to gray hematite is found in fumaroles in Alaska (see Section 3.3).

Minitti et al. (2002a, 2002b) have produced thin coatings of gray hematite by oxidizing synthesized basalts in terrestrial air at 700 °C from 1–7 days. These coatings reproduce some of the spectral features that characterize the hematite deposits on Mars. Thus, near-instantaneous oxidation of pyroclastic glass during emplacement may be a possibility for formation of gray hematite. However, there are several issues to bear in mind when considering this otherwise attractive hypothesis:

(1) Terrestrial air with 0.21 bar of O_2 and high absolute amounts of water vapor is not a realistic chemical analog for the current martian atmosphere, which has $\sim 27{,}000$ times less oxygen, $\sim 7.9 \times 10^{-6}$ bar O_2, i.e., 0.13% of ~ 6.1 mbar martian mean surface pressure (Owen, 1992).

(2) The early martian atmosphere, if anything, would have been even more anoxic due to active volcanism on early Mars (see Section 7), noting that active volcanism is obviously necessary to produce pyroclastics in the first place.

(3) If the process required were merely atmospheric oxidation of basalt, one would expect specular hematite to be common on Mars but it is not. An alternative possibility suggested by Minitti et al. (2002a) is that post-emplacement heating by later hydrothermal activity produced the gray hematite, which is a mechanism favored in this paper.

Tanaka et al. (2000), Noreen et al. (2001), and Hynek et al. (2002) have postulated that the martian gray hematite to iron ore deposits may be like those found in El Laco, northern Chile. As we discuss below, the way that the El Laco deposit formed is controversial and much of the evidence points to a hydrothermal origin rather than in-air oxidation of ash or direct volcanic ascent. Moreover, most of the iron ore is magnetite. Some literature attributes such iron ores to direct ascent from volcanism (Park, 1961) but as discussed previously, this idea is irreconcilable with thermodynamics given the plausible range of oxygen fugacities

in magmas. Such iron oxide ores are generally characterized by the assemblage magnetite–hematite–apatite (Fe_3O_4–Fe_2O_3–($Ca_3(PO_4)_2$)). From subsurface to surface levels in drill cores, ore varieties follow the order: low-P ($< 1\%$) magnetite–hematite, P-rich ($> 1\%$) magnetite–hematite, and P-free hematite (Parak, 1975). Other examples of the locations of iron ores similar to El Laco include Iron Springs in Utah and Kiirunavaara in northern Sweden. Such ores are generally termed "Kiruna type ores" after the latter location. These iron ores are thought to form when the main part of a volatile-rich magma crystallizes, leaving a water-rich melt that is ejected as a late phase with hydrothermal activity. There is much debate about whether Kiruna ore bodies show the presence of a "magnetite lava" (Nyström and Henríquez, 1994) or whether the magnetite is a hydrothermal replacement mineral. For example, the latter view is favored by Parak (1975) and Bookstrom (1995). Recent work shows that the late stage ores at El Laco, such as hematite, most probably derive from hydrothermal activity (Foose and McLelland, 1995; Bookstrom, 1995). In particular, hypersaline aqueous fluids boiling at around 250–350 °C are implicated (Sheets et al., 1997). This view is supported by fluid inclusion and isotopic evidence work, interpretation of contact relations between ore and host rock, and other field observations (Oreskes et al., 1994). Fluid inclusions contain soluble chlorides and anhydrite indicating fluid alteration of the andesitic host rock at El Laco.

Oxidation of magnetite ($Fe_2^{3+}Fe^{2+}O_4$) to hematite (solely Fe^{3+}-bearing) in Kiruna-type ores is incomplete, so we might expect to see TES spectral evidence of magnetite on Mars if the gray hematite deposits are analogous to Kiruna-type ores but we do not. We can see that complete oxidation is difficult by examining the equilibrium chemistry. Oxidation of magnetite to hematite can occur hydrothermally via

$$2Fe_3O_4 + H_2O = 3Fe_2O_3 + H_2. \tag{1}$$
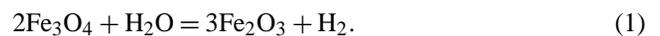
However, the production and buildup of H_2 inhibits this reaction proceeding to the right, so the only way that the reaction can proceed is if H_2 is continually removed from the reaction zone either by diffusion or by being carried in solution. From the stoichiometry of (1), it is necessary to remove 2 g (1 mole) of H_2 for every 462 g (2 moles) of magnetite that is oxidized, which translates to 4.3 milligrams of H_2 for every 1 g of magnetite. If water removes H_2 in a subsurface environment, the partial pressure of H_2 and therefore the amount that can be carried away will be controlled by the oxygen fugacity of the fluid, which is set by the mineral assemblage. Suppose the magnetite in a terrestrial Kiruna-type ore had been oxidized in a very deep environment before emplacement, around 600 °C and 5 kbar (~ 18 km) depth. Under these pressure–temperature conditions, hydrogen fugacity, f_{H_2}, is about 0.04 bar at the magnetite–hematite buffer, which gives a partial pressure $P_{H_2} = f_{H_2}/\gamma_{H_2} = 0.013$ bar where $\gamma_{H_2} \approx 3$ is an activity coefficient at the given pressure–temperature conditions. Consequently, hydrogen can only reach a concentration in

water of $P_{H_2}/P_{H_2O} = 0.013/5000 = 2.6$ ppm, or 0.26 mg per 100 g of water, where we assume that the water attains lithostatic pressure at depth, as is commonplace (e.g., Fyfe et al., 1978). So to remove 4.3 milligrams of H_2 and replace 1 g of magnetite with hematite requires $(4.3/0.26) \times 100$ g $= 1600$ g water per 1 g of magnetite, which is a tremendous amount of water. At lower temperatures and shallower depths, even more water is required. For example, at 230 °C and 0.5 kbar (1.8 km) depth, $f_{H_2} = 1.3 \times 10^{-4}$ bar and $\gamma_{H_2} \approx 1.1$, giving $P_{H_2}/P_{H_2O} = 2.4 \times 10^{-7} = 0.024$ g per 100 g of water, which requires 17.9 kg of water per 1 g of magnetite for complete replacement of magnetite by hematite. There are two alternatives to such an excessive water flux: first, that oxidation occurs as a non-equilibrium near-surface hydrothermal process whereby H_2 can easily diffuse and escape; second, that oxidation from meteoric water with dissolved O_2 occurs. Both ideas are consistent with the highest degree of oxidation being closest to the surface at El Laco (Broman et al., 1999). Meteoric waters are oxidizing because of Earth's O_2-rich atmosphere, which arises because of Earth's photosynthetic biosphere. This is perhaps a good reason why the occurrence of hematite in Kiruna type magnetite ores is a poor analog for the martian hematite. However, the lack of a spectral signature for associated magnetite on Mars is probably the most definitive evidence arguing against any direct similarity, because magnetite is by far the dominant mineral in Kiruna-type ores, however they may form. Some of the Kiruna-type magnetite always has a massive, crystalline expression, so it seems unlikely that magnetite associated with coarsely crystalline hematite on Mars might somehow always be very fine grained, behaving like a blackbody without a clear TES spectral signature.

3.2. Hematite formation in sedimentary environments

3.2.1. Sedimentary deposits of coarse-grained crystalline hematite

Given the potential similarities between early martian and terrestrial geochemistry, Burns (1993) postulated that banded iron formations (BIFs) may have been a feature of early episodes of water on Mars, an idea later explored by Schaefer (1996). Consequently, the question arises, could BIFs be responsible for martian gray hematite? BIFs are laminated sedimentary rocks containing $\geqslant 15$ wt% iron, with alternating iron-rich and iron-poor (usually silica-rich) layers. Specularite occurs frequently in terrestrial BIFs (see below). In order to understand whether BIF formation of gray hematite is plausible for Mars, we need to consider how gray hematite actually formed in terrestrial BIFs. The possibility that gray crystalline hematite on Mars might be similar to gray crystalline hematite found in some terrestrial BIFs is also potentially interesting because the precursor iron oxides in terrestrial deposits are widely attributed to the action of the early biosphere (Cloud, 1973, 1988; Allen et al., 2001).

First, we consider how the initial iron oxide sediment in BIFs was formed with a view to considering whether some-

thing analogous could have occurred on Mars. In the consensus model of terrestrial BIF genesis, ferrous iron (Fe^{2+}) was exhaled into Earth's early oceans from seafloor vents and circulated to the continental shelves where it was oxidized and deposited (Holland, 1984; Beukes and Klein, 1992). In standing bodies of water, iron precipitates as finely-divided reddish hematite, not as gray crystalline hematite. There are three ways in which the iron could initially be precipitated:

(1) chemical oxidation,
(2) photo-oxidation, and
(3) biological oxidation.

We discuss these processes in turn before describing how the fine-grained hematite gets transformed to coarsely crystalline hematite.

Chemical oxidation. On the basis of observation (Cornell and Schwertmann, 1996), oxidation of ferrous iron in solution proceeds via an intermediate phase of ferrihydrite, "$Fe(OH)_3$," an amorphous, insoluble red–brown gel

$$4Fe^{2+} + O_2 + 10H_2O = 4Fe(OH)_3 + 8H^+. \tag{2}$$
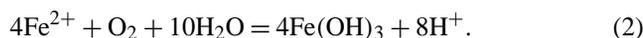
Ferrihydrite is unstable and converts irreversibly to goethite (α-FeOOH)

$$Fe(OH)_3 = FeOOH + H_2O. \tag{3}$$

This, in turn, may convert to hematite (α-Fe_2O_3) via

$$2FeOOH = Fe_2O_3 + H_2O, \tag{4}$$

depending on environmental conditions and the presence of other species in solution. Hematite may form directly from ferrihydrite, competing with goethite. In general, goethite formation is favored in alkaline solution at moderate temperature. Hematite is dominant near neutral pH and higher temperatures (Fischer and Schwertmann, 1975; Johnston and Lewis, 1983). The oxidation rate increases by $\times 100$ per unit pH but is slower in more saline water (Millero et al., 1987).

Photo-oxidation. Others have suggested that the iron oxide in BIFs was abiotically photo-oxidized (Braterman et al., 1983). In certain solutions, the photo-oxidation process starts with the formation of an iron complex and iron is oxidized by the photo-stimulated release of hydrogen gas:

$$Fe^{2+} + H_2O = [Fe(OH)]^+ + H^+,$$

$$2[Fe(OH)]^+ + 2H^+ + h\nu \rightarrow 2Fe(OH)^{2+} + H_2,$$

$$Fe(OH)^{2+} + 2H_2O \leftrightarrow Fe(OH)_3 + 2H^+.$$
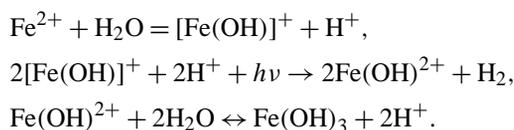
The absorption peak is in the ultraviolet ~ 250 nm. With aging, ferrihydrite converts to hematite via Eqs. (3) and (4). Thus even in a completely anoxic atmosphere, it is theoretically possible to oxidize Fe^{2+} and produce iron oxides. However, the absence of precambrian BIFs on very shallow

water platforms in the photic zone (where sunlight penetrates) and their presence at greater depth, makes the photo-oxidation hypothesis very unlikely (Des Marais, 1994). Instead, geological observations favor the view that the photic zone was oxidizing due to the action of microbes, and that perhaps a mobile oxidant, O_2, penetrated beneath the photic zone to oxidize Fe^{2+}. In addition, evidence for oxygen-producing photosynthetic bacteria on early Earth since at least 2.7 Ga (Brocks et al., 1999) renders the photo-oxidation hypothesis superfluous for post-2.7 Ga BIFs. There is also a problem in the UV hypothesis with silica. Silica is expected to accompany iron because if iron is leached out of basaltic rocks dissolved silica dissolves also. For example, acid weathering of pyroxene can be represented as

$$FeSiO_3 + 3H_2O + 2CO_2 = Fe^{2+} + 2HCO_3^- + Si(OH)_4.$$
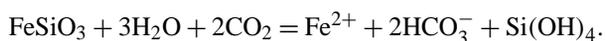
Silica is therefore expected to have been close to saturation in Earth's early oceans, unlike today's oceans where microorganisms that build siliceous shells suppress dissolved silica abundance by taking it out of the water (Siever, 1992). Recent laboratory studies show that in silica-rich waters, spontaneous flocculation of iron–silicate gels prevents the photo-oxidation of iron. In other words, this precipitation seems to lower iron concentrations sufficiently that the effects of photo-oxidation are minimal (Hamade et al., 2000; K. Konhauser, private communication). Thus photo-oxidation of iron has not been shown to occur in realistic multi-element solutions close to neutral pH. Thus there is reason to doubt that the photo-oxidation of iron suggested by Burns (1993) and Schaefer (1996) for early Mars is realistic. This means that if we entertain the idea of BIFs on early Mars, we should consider a mechanism for the direct oxidation of ferrous iron.

Biological oxidation.   Many researchers believe that in the initial sedimentary deposition of ferric iron in BIFs, microbes provided the oxidizing power to change soluble Fe^{2+} to insoluble Fe^{3+} (Cloud, 1973, 1988; Walker, 1987). Recently, it has been suggested that some purple bacteria can couple Fe^{2+} oxidation to the reduction of CO_2 during anoxygenic photosynthesis (e.g., Widdel et al., 1993; Heising et al., 1999) via

$$4Fe^{2+} + CO_2 + 11H_2O + bacteria$$
$$\rightarrow CH_2O + 4Fe(OH)_3 + 8H^+.$$
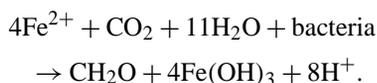
This process may have been responsible for iron deposition on the early Earth, before free oxygen became widely available as an oxidant (Ehrenreich and Widdel, 1994). However, BIFs tend to be very poor in organic carbon, so in this scenario, the organic carbon has to be efficiently recycled by biota and lost as a volatile species such as CH_4, in a concept similar to that suggested by Walker (1987).

The hematite formed in all of the three sedimentary oxidation processes discussed above (chemical oxidation,

photo-oxidation, and biological oxidation) is in the reddish, finely divided form. We argue below (Section 3.3) that temperatures $\sim 100\,°C$ or more are needed to form large (several microns) platy hematite crystals. To convert sediments to lithified BIFs, fine-grained iron oxide sediments that originally formed as described above on ancient continental shelves on Earth were later altered at depth by burial metamorphism or hydrothermal activity (or both). Thermal processing converted microcrystalline or amorphous iron oxides to coarse-grained crystalline hematite (Powell et al., 1999; Barley et al., 1999; Taylor et al., 2001).

The potential relevance of this discussion of BIFs to Mars is two-fold:

(1) If the original iron oxide that acted as a precursor to the martian crystalline hematite was deposited in a standing body of water, a sufficient source of oxidizing power was required.
(2) The gray crystalline hematite in terrestrial BIFs results from low-grade metamorphism and/or hydrothermal recrystallization of precursor minerals like small-grained goethite, hematite or magnetite; so any comparison to Mars must also consider how such physical and chemical conditions for thermal transformation occurred on Mars.

That thermal transformation is needed is borne out by terrestrial field observations. A study of Permian–Triassic iron ore deposits in the Sierra Nevada near Granada, Spain, suggests that pre-metamorphic oxide facies of microcrystalline hematite and goethite recrystallized to specularite during metamorphism (Torres-Ruiz, 1983). Bischoff (1969) estimated that a temperature $\sim 140\,°C$ is needed to transform goethite (α-FeOOH) to hematite (α-Fe_2O_3) by dehydroxylation (provided the goethite precursor is sufficiently coarse-grained (Langmuir, 1971)). This is consistent with temperatures deduced for the formation of coarse-grained hematite in the best-preserved ancient terrestrial iron formations. Specularite (with 50–100 μm-sized platy crystals) in the Dales Gorge Member of the Brockman Formation, part of the Hamersley Range in Western Australia, formed at temperatures $\sim 140\,°C$ on the basis of oxygen isotopes (Becker and Clayton, 1976). This temperature is consistent with the estimated maximum temperature of 205–325 °C from an estimate of the burial depth of the Dales Gorge Member and assuming a geothermal gradient of 15 °C km^{-1}. Similarly, oxygen isotope data for parts of the Bibawik Iron Formation in northern Minnesota, indicate formation temperatures $\sim 150\,°C$ (Perry et al., 1973). Indeed, as noted by Chaudhuri (1967), in all known cases of the occurrence of specularite in bedded sedimentary deposits there has been heating of the original primary sediments. If the origin of the coarsely crystalline hematite on Mars started with aqueous deposition in a standing body of water, this must have been followed by either deep burial up the geothermal gradient or some other large-scale thermal perturbation due to igneous activity, such

as contact metamorphism. The general response to burial up the geothermal gradient is dehydration and an increase in crystal size, that is, recrystallization. We return to this idea latter to set some quantitative constraints for how deep martian red oxide sediments would need to be buried to convert to gray hematite (Section 4).

3.3. Hematite formation in hydrothermal environments

3.3.1. Coarse-grained crystalline hematite from hot waters

Newly formed chemical sediments tend to be composed of fine-grained material. Small crystals have larger vapor pressures and greater solubility than larger crystals (e.g., Cornell and Schwertmann, 1996, p. 199). Thus, the response to heating processes is grain growth because at higher temperatures, bigger crystals are more stable (e.g., Laudise, 1970). Also, when a $Fe(OH)_3$ gel is formed from oxidation of iron at warm temperatures (i.e., closer to $100\,^\circ C$ rather than room temperature), there tend to be more hematite nuclei present, which leads to large hematite platelets (several microns or tens of microns) in subsequent aging to coarse hematite crystals (Sugimoto et al., 1996). The crystal size and shape determines whether the infrared spectrum is likely to conform to that observed on Mars by TES with spectral absorption features at 450 and 560 cm^{-1} (Christensen et al., 2000; Lane et al., 2002b). The key point is that at temperatures close to room temperature or below, the formation of hematite crystals of several microns size or larger is not favored.

Several laboratory studies have investigated the formation of crystalline hematite from hydrothermal solutions. Early investigations of the system Fe_2O_3–H_2O found that crystalline hematite was favored at high temperatures $> 130\,^\circ C$ (Schmalz, 1959) or $> 80\,^\circ C$ (Vorobyeva and Melnik, 1977), with the exact value depending on pH and pressure. For commercial purposes (pigments and anticorrosive coatings in paints), crystalline hematite is generally hydrothermally synthesized at around ~ 150–$200\,^\circ C$. Synthesis typically utilizes the hydrothermal transformation of ferrihydrite (Eqs. (3) and (4)), where a variety of solutions control particle shape and size (e.g., Kolb et al., 1973; Cornell and Schwertmann, 1996, pp. 492–493; Diamandescu et al., 1999).

3.3.2. Solution chemistry and why sulfate is an unlikely oxidant

In natural systems, saline Cl-rich hydrothermal solutions are capable of carrying large amounts of iron complexed as $FeCl_3$. Indeed, experimental studies confirm this and show that iron chloride complexes limit other cations to relatively low abundance (Crerar et al., 1985). The hydrothermal precipitation of iron oxides is likely caused by the decrease of temperature and pressure when fluids migrate upwards into a more oxidizing environment, in part because the solubility of Fe in hydrothermal solutions is positively correlated with temperature (Barnes, 1979; Kwak et al., 1986).

In principle, sulfate-rich fluids could also be an oxidizing agent for iron and produce hematite. However, if sulfate is used as an oxidant for $Fe^{2+} \rightarrow Fe^{3+}$ then the sulfate must be reduced to sulfide to satisfy redox balance. This means that we would observe hematite accompanied by sulfide minerals. The mineral assemblage of hematite and sulfide is very uncommon in terrestrial rocks because of the unlikely mixed oxidation state. On Mars, there is no spectral detection of stoichiometrically-balanced sulfide with the hematite (S. Ruff, private communication), so there is no evidence to suggest that sulfate was the original oxidant. In contrast, if water had been the oxidant, volatile H_2 would have been lost from the mineral assemblage.

3.3.3. Coarse-grained crystalline hematite from vapor phase iron and water vapor

Specular hematite is known to occur around (hydrothermal) fumaroles in various places around the world: for example, at Stromboli and Vesuvius in Italy and the Valley of Ten Thousand Smokes in Alaska. In the latter case, fumaroles developed on hot ash-flow tuff that fell on top of the water and ice of preexisting rivers, lakes and glaciers (Keith, 1984). In the early 19th century, the famous French chemist Gay-Lussac synthesized specularite from $FeCl_3$ vapor upon contact with water vapor at a high temperature in an attempt to simulate such fumarolic specular hematite deposits (Gay-Lussac, 1823). Ferric chloride has a high vapor pressure above $200\,^\circ C$ and is readily transported in the vapor phase (Zies, 1929). After delivery to the surface, ferric chloride can react with water vapor and form hematite, as follows:

$$2FeCl_3(g) + 3H_2O(g) = Fe_2O_3(s) + 6HCl(g).$$
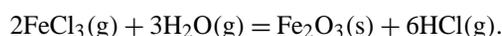
Such vapor phase reactions are conjectured to be responsible for ash-like crystalline hematite found in iron oxide deposits around the Chupaderos caldera near Durango City, Mexico (Lyons, 1988).

Following up on Gay-Lussac's work, Martin and Piwinskii (1969) showed that iron could be leached from andesite and diabase using pure water at 1.25–10 kbar, a 2 : 1 water : rock ratio, and temperatures of $700\,^\circ C$. In their hydrothermal experiments, iron was transported as a vapor, leading to platy hematite nucleation and crystallization in a quenching "cold-trap" at $\sim 500\,^\circ C$. The presence of a melt, or of chloride, fluoride, sulfide or carbonate ions was not necessary for the leaching of iron and transport of iron as a vapor in Martin and Piwinskii's experiments. Of course, given that the lithostatic pressure on Mars only increases only $\sim$ a few $\times 10^2$ bar per km depth, the pressures in Martin and Piwinskii's experiments are inapplicable for a plausible near-surface geological environment on Mars. However, these experiments are an interesting variant on a hydrothermal means to form specular hematite. Certainly, some platy hematite deposits observed in the field appear to coat and grow on surfaces of other minerals and much resemble vapor-deposited material.
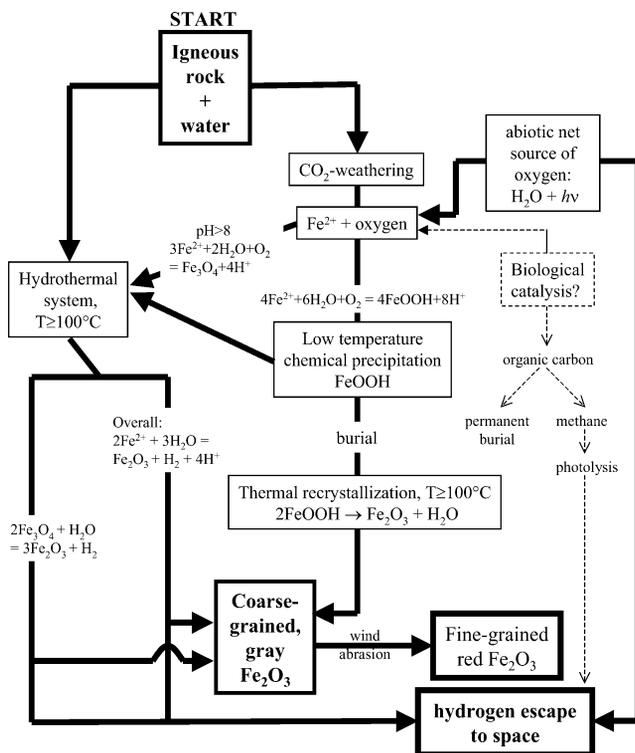
Fig. 1. Chemical pathways for the formation of gray crystalline hematite. Two main routes are shown: (1) low-temperature precipitation followed by hydrothermal processing; (2) direct hydrothermal formation. Redox balance requires that the production of an oxidized species, hematite, be balanced by stoichiometric amounts of reductant, such as hydrogen. A dashed sub-pathway shows the likely effect of microbial biology, if it ever existed on early Mars.

3.4. Summary of the chemical pathways to form gray, crystalline hematite

Figure 1 summarizes the possible chemical pathways to form gray, crystalline hematite, on the basis of its terrestrial occurrence and its laboratory synthesis, as reviewed above. The figure identifies the chemistry of two main pathways:

(1) Low temperature oxidation of iron and precipitation of iron oxides in a standing body of water with subsequent burial and thermal recrystallization to gray hematite.
(2) Direct hydrothermal formation of the coarse-grained hematite.

4. Thermal constraints for the formation of gray crystalline hematite

It is obvious from all of the above that there is one common environmental variable for the formation of coarse-grained crystalline hematite: a warm temperature. We now calculate that temperatures in excess of about 100 °C are required for the recrystallization of hematite from small-grained iron oxide precursors like goethite.
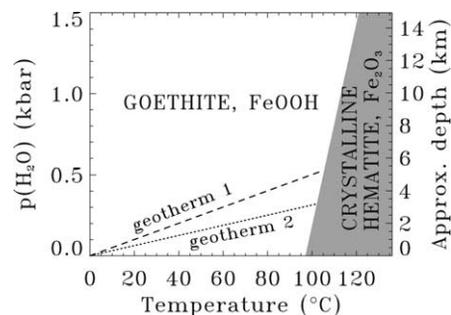
Fig. 2. Stability fields of goethite and hematite as a function of temperature and H_2O pressure. For most geological situations the latter can be taken as being approximately equal to the lithostatic pressure. On the right, the equivalent subsurface depth is shown. At depth, hydrous iron oxides (typified by goethite) recrystallize to coarsely crystalline hematite due to heating. Two possible geothermal gradients for early Mars are shown to illustrate the range of uncertainty on this calculation. Geotherm 1 (dashed) corresponds to an early heat flux of $50\ \mathrm{mW\,m^{-2}}$, while geotherm 2 (dotted) corresponds to a heat flux of $80\ \mathrm{mW\,m^{-2}}$.

Let us consider the case where iron oxides are deposited from solution, buried, and then recrystallized to form gray hematite. Fresh sediments typically contain about $\sim 50\%$ water, which is squeezed out during burial as pore water is eliminated. Consequently, at moderate depths, the water is either bound in chemical compounds or adsorbed onto the grains of sediments like iron oxides. All such compounds consisting of a combined volatile and solid phase exert a vapor pressure as a function of temperature, pressure, and grain size. At moderate depth, porosity and permeability are small and fluids "fight" their way out, which yields the approximate assumption that the pore–fluid pressure approaches the lithostatic pressure. Thus iron oxide dehydration and hematite recrystallization will occur at a depth where the geotherm intersects the dehydration line for bound water.

Figure 2 (the basis of which is described below) shows the theoretical calculated boundary between goethite and hematite as function of temperature and pressure using thermodynamic data from Diakonov et al. (1994). The calculation is supported by data: At low pressure, various workers have reported a temperature of 70–130 °C for the decomposition of goethite to hematite in the presence of saturated water vapor (Schmalz, 1959; Wefers, 1966; Vorobyeva and Melnik, 1977; Johnston and Lewis, 1983). (Note that this transition temperature differs from the dehydration temperature of ~ 250 °C required to change goethite powder to hematite under dry conditions (Pollack et al., 1970; Morris and Lauer, 1981); in the aqueous system, crystal growth effects lower the transition temperature.) In Fig. 2, as temperature increases, hematite becomes the more stable phase. However, an increase in pressure does not help the dehydroxylation process (Eq. (4)) because it acts thermodynamically to oppose the conversion to hematite by Le Chatelier's principle. Hence the stability line has a positive slope. Thus, at higher pressure (greater depth) a greater temperature is required for recrystallization.

To estimate a geothermal gradient requires knowledge of the heat flow and the thermal conductivity in the subsurface. Theoretical models of the heat flow suggest that the global-mean surface heat flow on Mars is in the range of 20–45 mW m^{-2} for the present day (see Schubert et al. (1992, 2001) for reviews). An intermediate value of ~ 30 mW m^{-2} is commonly used. It is generally believed that the heat flow was higher on early Mars, but estimates range widely from a value similar to the present heat flux to ~ 100 mW m^{-2} (Schubert et al., 1992). Thermal conductivity is also uncertain on Mars. Most minerals, including basalt, have conductivity ~ 4.5 W m^{-1} K^{-1} (see Roy et al., 1989). However, compositional interfaces, crystal imperfections, and the filling of voids with ice will tend to reduce the conductivity. Consequently, Clifford (1993) suggested a value of 2 W m^{-1} K^{-1} while Mellon and Jakosky (1995) favored 3 W m^{-1} K^{-1} for the martian megaregolith. We adopt an intermediate value of 2.5 W m^{-1} K^{-1}. Thus, in Fig. 2, a nominal early Mars geothermal gradient (dashed line) is shown assuming a heat flux of 50 mW m^{-2} and conductivity of 2.5 W m^{-1} K^{-1}. This intersects the stability field of hematite at about 5-km depth. Consequently, iron oxide sediments would be expected to recrystallize at this depth to form crystalline hematite. This depth could be smaller if we use a geothermal gradient for early Mars that is larger than our assumed 50 mW m^{-2}. For example, a geothermal heat flux on early Mars of ~ 80 mW m^{-2} is an equally plausible possibility for 4 Ga, given the uncertainty of models (Schubert et al., 2001, p. 694), and would produce a larger geothermal gradient that would allow for a shallower recrystallization depth of ~ 3 km (Fig. 2). Nonetheless, this depth of burial still implies fairly drastic amounts of erosion by martian standards (3–5 km of overburden material) to re-expose deposits of crystalline hematite. Alternatively, recrystallization would occur at very shallow depths if tens to hundreds of meters of hot impact ejecta melt were to cover the surface as a result of a large impact on early Mars. The heat released from such a large accumulation of melt would generate a downward thermal pulse and a thermal gradient such that temperature would decrease with depth from the surface. Eventually, the thermal profile would reach a point of inflection with a gradient reversal, such that it would smoothly join the geothermal gradient at depth (see Sleep and Zahnle, 1998). The ~ 2500-km diameter Hellas impact crater produced an ejecta blanket of about 70 m depth if globally averaged (Sleep and Zahnle, 1998), so very large impacts produce massive amounts of melt. Smaller impactors could produce similar or greater depths of ejecta if the ejecta blanket were regionally confined. The smaller the source crater, the thinner the ejecta blanket, and the closer to the surface hematite would crystallize, down to approximately twice the ejecta blanket depth. Thus knowledge of the vertical extent of the hematite could set constraints on this possibility. In Aram Chaos, it appears that the hematite is detected over an elevation range of order $\sim 10^2$ m (see Section 6). We do not know if this represents the actual depth of the deposit or merely a smearing out of a thin deposit by erosion. Also the deposit is below the highest topographic level and was buried at least a few hundred meters. Thus, taken at face value it seems unlikely that the source of heat came from above. Geothermal heat from below seems more likely to have caused the formation of gray hematite. Hematite could also result from hydrothermal systems induced by impact structures, although in the Canadian impact structures, the hematite is mostly the red variety (Phinney et al., 1978; Morris et al., 1995). However, impacts into the hematite deposits on Mars, once they had formed, may have created local effects in surrounding ejecta debris. Bolides that have impacted the hematite deposits will likely have created hematite impact bombs, i.e., aerial recrystallization of melted material. Such a phenomenon occurs on Earth. In the 40-km diameter Araguainha astrobleme, in central Brazil, where a bolide impacted Fe-rich sedimentary rocks, aerial melt segregation led to impact bombs of 2–50 cm size composed of pure hematite crystals 50 μm to 3 cm in size (Hippert and Lana, 1998). The influence of impacts should therefore not be ignored if the geology of hematite-rich rocks is viewed in detail from future landers or rovers on Mars.

5. Regional geological settings of the crystalline hematite deposits

In order to draw conclusions about the formation of the gray hematite on Mars, it is useful to take into consideration the geological context of all occurrences of gray hematite. Thus, we briefly review the geology of the Sinus Meridiani and Vallis Marineris deposits. We also introduce the geology of Aram Chaos before presenting more detail on this region in the next section.

5.1. The Meridiani Formation

Edgett and Parker (1997) first described the geomorphology of the location of the largest gray hematite deposit, Sinus Meridiani, based on ~ 30 m pixel^{-1} Viking Orbiter imaging. They noted a smooth deposit embaying, thus superposed, on a moderately valley-dissected surface outcropping to the south. Order-of-magnitude higher resolution MOC imaging indicates that this unit is smooth, with layers and mesas forming outliers of a largely stripped overlying deposit, and that the unit has internal layering where exposed along its eroded margin (Christensen et al., 2001; Malin and Edgett, 2001). The geomorphic presentation of the erosion of the hematite-bearing unit, as well as the remnants of the unit superposed upon it, has led Christensen et al. (2001) to conclude that these materials are sedimentary and have undergone physical weathering by the wind over geological time. Deep infrared absorption features of basalt, the dominant host rock for the gray hematite material, suggests that the individual basalt grains of the deposit are at least sand sized, implying that the deposit was unlikely to

originate as air-fall (Christensen et al., 2001). The absence of a hematite signature in a 22-km-diameter crater along the southern periphery of the deposit is taken to refute the possibility that the hematite is simply a wind-introduced surface mantle and to infer an in-place rock unit that is thinner than the excavation depth ($\sim$ 2 km) of the crater (Christensen et al., 2001). Christensen et al. (2001) conclude that the hematite-bearing unit in Sinus Meridiani was previously more extensive, has undergone erosional stripping by the wind, and once eroded, became mobile and dispersed, given that none is detected on the surrounding surfaces. Christensen et al. (2001) note that the hematite constitutes the first rock-stratigraphic unit identified by mineralogical composition on Mars, which they name the Meridiani Formation.

5.2. Vallis Marineris

Christensen et al. (2001) also report numerous small (5–20 km) areas in Vallis Marineris exhibiting the spectral signature of gray hematite, with the most extensive outcrops within Candor and Ophir Chasma. Though they found the exact locations of these areas difficult to determine, they conclude that the hematite-bearing materials are associated with dark material located in topographic lows located near well-known eroded layered deposits. Gray hematite is apparently absent in regions of Vallis Marineris that do not exhibit interior layered deposits, so that gray hematite formation appears invariably directly associated with layered materials.

5.3. Aram Chaos

Christensen et al. (2001) also report the presence of a gray hematite zone in the north–east quadrant of Aram Chaos. Aram Chaos (21°W, 2°N) is an isolated area of chaotic terrain contained completely within an eroded and largely in-filled crater. It forms part of the larger occurrence of chaotic terrain to the east of Vallis Marineris between 10 to 50°W and 20°S to 10°N. Chaos regions on Mars are areas where jumbled arrays of blocks have apparently been produced by collapsed ground. Chaotic terrain (and several box canyons) serve as the source regions for large out-flow channels that generally flow northwards and converge in the northern lowlands, principally Chryse Planitia. We now examine the geology and topography of Aram Chaos in some detail.

6. The geology of the gray hematite zone in Aram Chaos

Figure 3(a) shows a topographic map of Aram Chaos based on Mars Orbiter Laser Altimeter (MOLA) data (Smith et al., 2001). On the right, an outflow channel from Aram Chaos region feeds into Ares Vallis, which drains towards the northern plains. Figure 3(b) shows the same MOLA map with an overlay of the region enriched in coarse-grained crystalline hematite. Here the color denotes the "hematite index" exactly as defined by Christensen et al. (2001), which

is based on the depth of the spectral absorption features of gray hematite in TES spectra.

On Fig. 3(a), four individual MOLA tracks are shown that cross over the hematite-enriched region. The elevation of these four tracks is plotted in Fig. 4. It can be seen that the spectral signature for the Aram Chaos crystalline hematite is typically confined between about −3000 m and −2500 m elevation relative to the martian geoid defined by the MOLA team (Smith et al., 2001). From comparison with Fig. 3(b), we deduce that the TES spectral signature is weak at elevations close to −3000 m and maximal around −2600 m. The individual tracks clearly show that hematite does not occur above about −2500 m elevation. For example, along track 3 an area of topography between 339.13°E and 339.24°E rises above −2500 m and there is a clear break in the hematite signal. Going from west to east along track 4, hematite does not appear until about 339.6°E where the topography falls below the −2500 m contour. Along track 1 hematite appears on west–east slopes at 338.5°E and 338.94°E, again when the elevation falls below the −2500 m threshold. Peak concentrations of hematite (colored red in Fig. 3(b)) occur at an elevation of approximately −2600 m. Such peak concentrations occur at 339.15°E along track 1 and 339.55°E along track 3 in Fig. 4, when comparing Fig. 3(b).

Thus the maximum concentration of gray hematite lies around −2600 m. This is equivalent to benches that are colored very light green in Fig. 3(a). We interpret the lesser concentrations of hematite found at elevations up to a few hundred meters below this level as most likely a lag deposit from physical weathering. A terrestrial analog for such detrital hematite is seen at the Pilot Knob specularite ore in Missouri, where a $\sim$ 60 m thick accumulation of specularite-rich boulders is found below the main ore deposit on the lower slope and foot of the Pilot Knob Mountain (Seeger et al., 1989). On geological timescales, wind erosion will grind down any detrital crystalline hematite on Mars into smaller red-colored particles, so a strong spectral signature of crystalline gray hematite probably indicates a relatively recent exposure and erosion, much like that suggested for Sinus Meridiani (Christensen et al., 2000; Hartmann et al., 2001). The visible and near-infrared spectral properties of martian dust are compatible with mixtures of palagonitic dust and small amounts of red hematite (Morris et al., 1989, 1997). Such red "dust" hematite, because of its small particle size and low concentration, would not tend to be detected by TES, as observed. We interpret the topography and TES data in Aram Chaos as showing a regional layer of crystalline hematite restricted in elevation. Alternatively, the hematite deposit could consist of successive layers confined between two relatively close depths whose difference is < 500 m. In any case, the hematite stratum lies below the top level of the topography and is sharply confined below −2500-m elevation, suggesting a partially buried planar deposit (with a small-angle regional dip to the west (T. Glotch, private communication)).
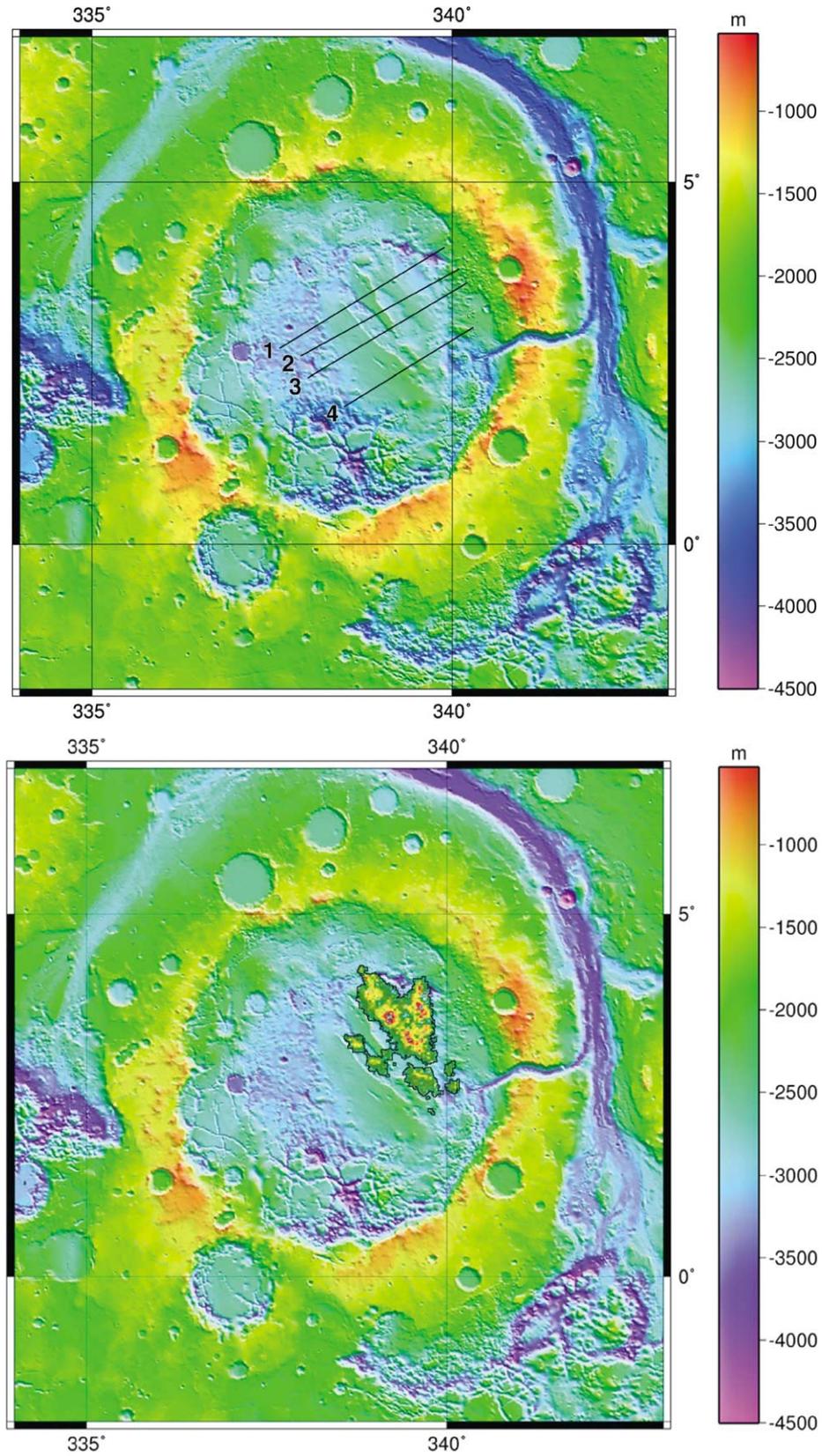
Fig. 3. (a) Aram Chaos topography contours from binned MOLA data. The four lines shown are individual MOLA tracks, which are also plotted in Fig. 4. (b) Aram Chaos topography with an overlay of the area enriched in coarse-grained crystalline hematite on the basis of spectral signatures from TES. The hematite signature is shown to match its graphic presentation in Plate 3 of Christensen et al. (2001).
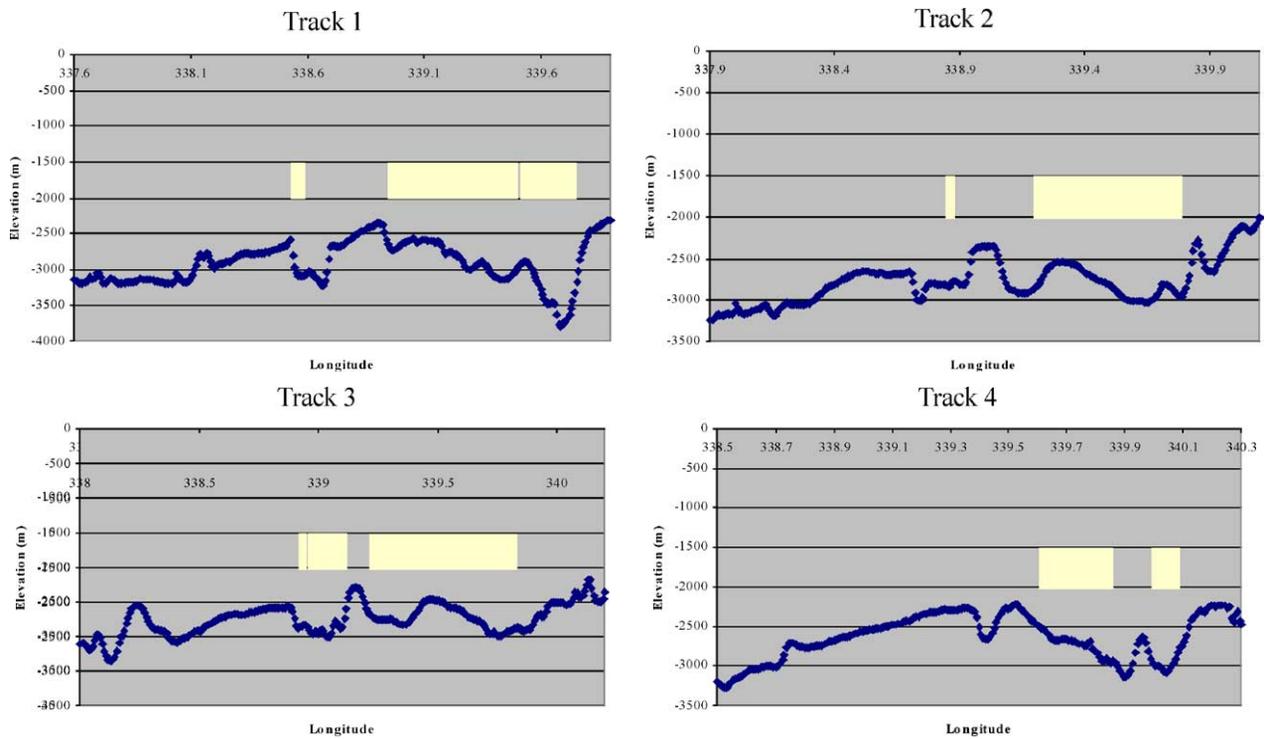
Fig. 4. MOLA track topography of the Aram Chaos hematite deposit. MOLA track numbers correspond to the track numbers on Fig. 3(a). The blocks above the topographic profile show the coincidence with the area of TES-detected hematite, as shown in Fig. 3(b).

Correlation of the gray hematite location in Aram Chaos with MOLA topographic mapping and imaging by the Mars Orbiter Camera (MOC) allows us to characterize the morphology and local stratigraphy of this material (compare Fig. 5 with Fig. 3). In Fig. 5, an image mosaic composed of MOC wide angle images (resolution ~ 250 m pixel^{-1}) shows that much of Aram Chaos' interior is surfaced by a prominent light-toned caprock. The major exposures of this caprock, such as that marked by the southernmost "C" in Fig. 5, appears heavily pitted and fluted in MOC narrow angle (NA) images. The subparallel orientation of this fluting implies that abrasion driven by strong unidirectional winds is the most likely agent. The boundaries of this capping deposit form scarps. Also scarp-bounded outliers of the caprock occur beyond the main outcrop (Fig. 6), which suggests that it was once more extensive. Bounding scarps of caprock material exhibit alternating benches and steps in MOC NA images, which we interpret to be due to the differential erosion of horizontal discrete layers, as did Christensen et al. (2001). In contrast to the main deposit, the upper caprock surface immediately above the hematite deposit, at least locally in the two examples shown in Figs. 6 and 7, is relatively smooth at the scale resolvable in MOC NA images. Perhaps this surface is composed of a lower, smoothly eroding layer within the caprock rather than the fluted exposures in the interior of the large outcrops.

In MOC NA images, the main gray hematite-bearing material appears to emerge from beneath the caprock (Figs. 6 and 7). The hematite deposit itself also shows alternating benches and steps, inferred to be an erosional expression of
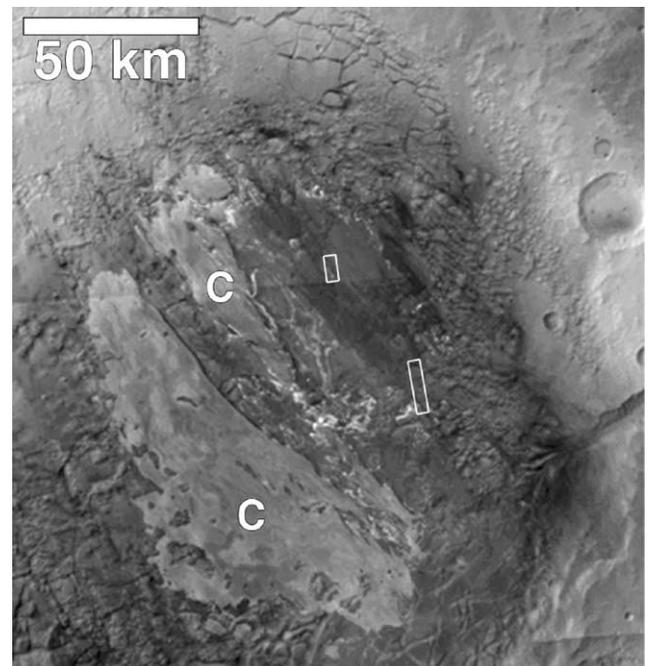
Fig. 5. Digital Image Map (DIM) of the interior deposits of Aram Chaos showing the locations of two MOC NA images of outcrops of the gray hematite found there. Figure 6 is located with the northern box and Fig. 7 is located within the southern and longer box. The hematite occurs under a widespread caprock (labeled "C") and thus is only exposed where this caprock has been striped back. (DIM produced from MOC red-filter Wide Angle images acquired during the "geodetic" campaign and assembled into "MC Quadrangle" charts using a simple cylindrical projection courtesy Malin Space Science Systems. Figure centered $\sim 3\,°$N, $21\,°$W. North at top. Illumination from left.)
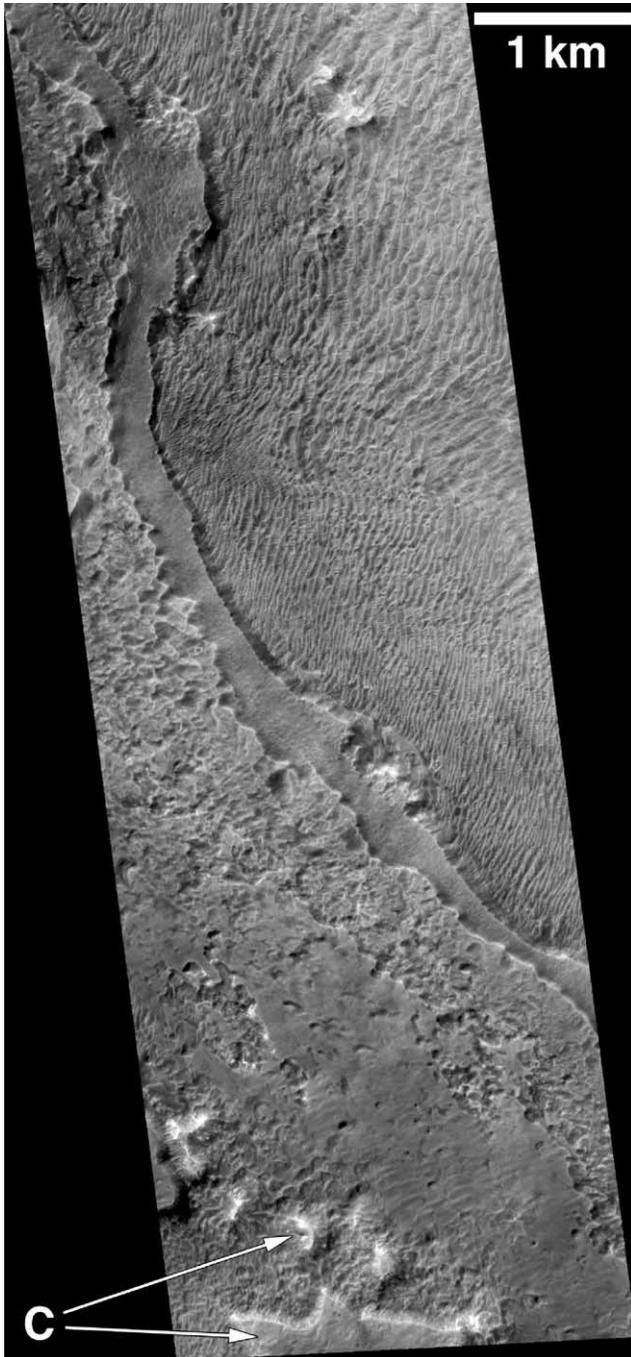
Fig. 6. The hematite-bearing unit dominates the lower-left-half of this figure. Beyond (upper right) and topographically below the hematite unit's bounding scarp is a "sea" of dune-forms (whether active, indurated or even possibly exhumed is undeterminable). Note that the hematite-bearing unit forms several scarps and benches, which are interpreted to be the result of differential erosion of several discrete layers. This differential erosion, presumably modern and due to wind-driven abrasion, has etched and pitted the tops of the benches. Small outliers of the brighter-toned and smoother caprock, which overlie the hematite baring unit, can be seen near the bottom of this figure (labeled "C"). (Portion of MOC narrow angle image M19-01361, centered at ∼ 3.5 °N, 20.6 °W, image-longitude-centered sinusoidal projection, original resolution 2.9 m pixel^{-1}. North at top. Illumination from upper left. Image processing courtesy Malin Space Science Systems.)
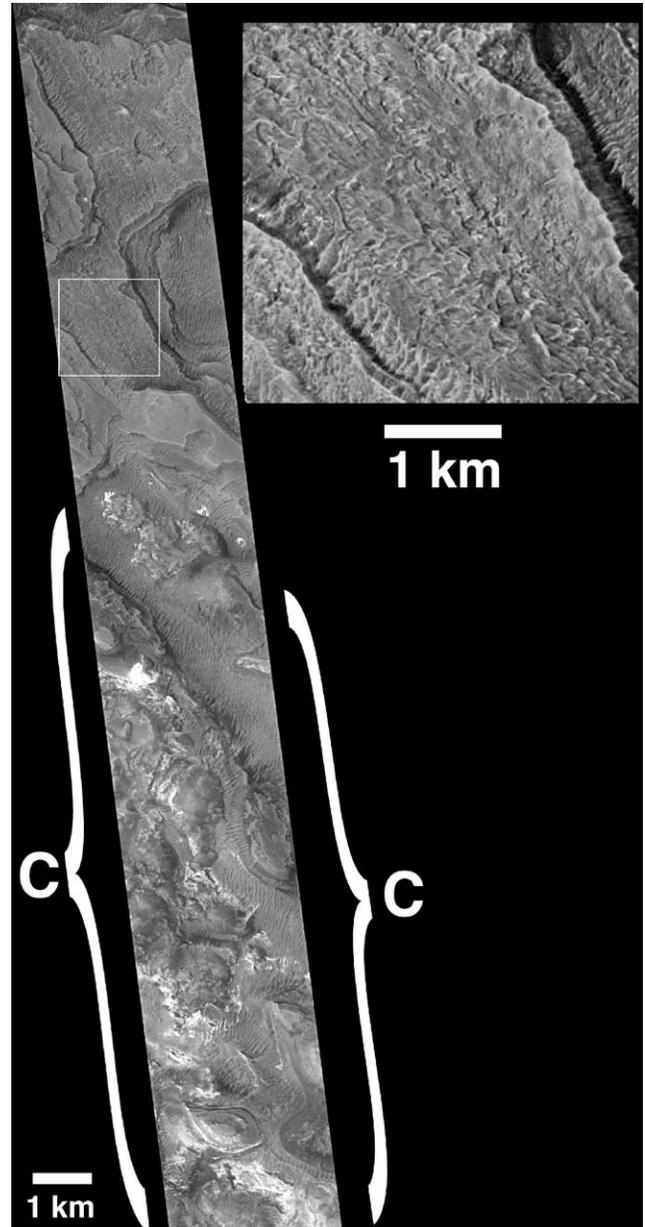
Fig. 7. The hematite-bearing unit outcropping beneath the caprock unit. Here also the hematite-bearing unit forms several scarps and benches interpreted to be layers. The inset at upper right shows that bench tops of the hematite unit here is etched and pitted. The brighter-toned and smoother caprock (labeled "C" between brackets), has eroded here to form step-and-bench buttes, strongly implying that it also is layered. Note that the erosion process does not etch and pit the caprock unit nearly to the extent it does the hematite unit. (Portion of MOC narrow angle image M09-06434, centered at ∼ 3.0 °N, 20.2 °W, image-longitude-centered sinusoidal projection, original resolution 4.4 m pixel^{-1}. North at top. Illumination from lower left. Image processing courtesy Malin Space Science Systems.)

layering. The hematite-bearing outcrops always appear to be heavily etched and pitted on decameter scales, with some fluting in MOC NA images. The layered hematite outcrops generally do not extend beyond 10–15 km of the last occurrence of the caprock, from which we speculate that it is more susceptible to erosion than is the caprock. It is reasonable to infer that the hematite-bearing rock is much more

extensive than its exposures, where protected by caprock. However, the lack of a hematite detection by TES west of the boundaries of the large caprock exposure (that marked by the southernmost "C" in Fig. 5) may mean that hematite is limited in the material beneath the caprock to the eastern portion of Aram Chaos. As the bulk of the hematite-bearing unit itself is composed of other minerals, i.e., those derived from basalt (Christensen et al., 2001), the unit may outcrop in western Aram Chaos and simply be devoid of hematite. Laterally beyond and topographically below the bounding scarps of the hematite-bearing rock outcrop is a surface ubiquitously covered by duneforms. There is a detectable, though weaker, presence of hematite in this "duneform" material. If the duneform material is indeed composed of relatively recently formed sand dunes whose sands were derived from the erosion of the hematite-bearing material, then the hematite-bearing deposit is probably not well consolidated and composed of individual sand-sized grains of predominantly basaltic composition. Presumably, the abrasion of sands in the dunes of the duneform material fairly quickly mutes or destroys the hematite signature. However, the evidence for the duneform deposit being stratigraphically superposed is not absolutely unequivocal. Alternatively these "dunes," if in fact that is what they are, could be "fossils" exhumed from beneath the hematite material. Fossilized duneform-textured surfaces are proposed for similar features elsewhere on Mars (Edgett and Malin, 2000a, 2000b; Malin and Edgett, 2001).

Groundwater release and structural failure of the overlying rocks is a plausible explanation for how the apparently collapsed ground of martian chaotic terrain formed (Sharp, 1973). Presumably, such release would be triggered by tectonic or geothermal activity. Thus the geology and topography of Aram Chaos is consistent with the formation of gray hematite due to the confinement and subsequent release of a hydrothermal aquifer. Possible terrestrial analogs are Proterozoic brecciated zones, such as in northern Yukon, Canada, and the Olympic Dam deposit in southern Australia (Thorkelson et al., 2001). At these terrestrial locations, breccia zones were generated by forceful explosions of volatile-rich fluids within the crust, most probably caused by igneous intrusions at depth. Rapid ejection of the hydrothermal fluids shattered large volumes of country rock. The Yukon breccia zones, collectively called Wernecke Breccia, cover an area 48,000 km^2 and are characterized by disseminated specular hematite (Thorkelson et al., 2001). Clasts and wallrocks were hydrothermally altered leading to metasomatic growth of specularite on the rims around clasts and in fractures. Zones of massive specularite are present in some Wernecke breccias. Hydrothermal activity at shallow subsurface levels similarly produced massive hematite in the Olympic Subdomain of the Gawler Craton in South Australia, although the geologic history in that region is somewhat more complex than in Yukon (Thorkelson et al., 2001). The gray hematite in Aram Chaos may have similarly had such a hydrothermal origin.

7. Redox considerations in the formation of gray hematite

The apparent unaltered composition of the basaltic surface of Mars contains iron as Fe^{2+}. Thus, no significant concentrations of hematite could have ever been produced without a concentrated source of oxidant to convert Fe^{2+} to Fe^{3+}. Possible candidates for the chemical oxidation processes are:

(a) direction aqueous oxidation with O_2 (or oxygen-bearing oxidants effectively redox-linked to O_2) produced abiotically in the atmosphere as a result of photo-dissociation of water,
(b) oxidation similar to Eq. (1) with H_2O that was dissociated as a result of hydrothermal activity,
(c) aqueous photo-oxidation, and
(d) biological oxidation.

Oxidation must be accompanied by the generation of a stoichiometrically balanced amount of reductant, as a fundamental matter of redox chemistry. In the case of (a)–(c), the reductant generated would be H_2, whereas in the case of (d) it would be organic carbon (or methane, if the organic carbon was metabolized). It is therefore worthwhile considering the redox chemistry necessary to produce the gray hematite on Mars in terms of the fate of the reductant that would have to be generated and the amount of oxidant needed.

7.1. Oxygen inventory in the gray hematite

In the sedimentary hypothesis for the formation of gray hematite on Mars (Section 3.2), direct oxidation in an aqueous environment with dissolved O_2 from the atmosphere is required. This may, on the face of it, seem reasonable given that the present martian atmosphere contains 0.13% O_2 due to photochemistry and is oxidizing (Owen, 1992). A net gain of oxygen to the planet is generated by the photo-dissociation of water and the subsequent loss of hydrogen to space, with overall reaction $2H_2O \rightarrow O_2 + 4H(\uparrow space)$. The escape process is the key step because otherwise hydrogen would photochemically recombine to form water, producing no net oxidation gain. Today, the O_2 in the martian atmosphere is significant from a redox point of view, but this predicament arises only because the losses of O_2 to chemical weathering of the surface and reactions with geothermal emissions of reduced gases are negligible. The sinks on O_2 are low because volcanism is (largely) extinct and a significant amount of liquid water is absent to catalyze surface oxidative weathering. In fact, these surface sinks are so low today that oxygen atoms are lost to space from Mars at a rate that is half of that for hydrogen atoms (McElroy, 1972; Liu and Donahue, 1976). Consequently, Mars is in a state of redox stagnation. One would deduce that Mars' red color (from oxidation) did not occur as a result of current processes on Mars; instead, the oxidation resulted because

early Mars must have been different with a greater escape rate for hydrogen than oxygen. Clearly, the excess oxygen in the Fe_2O_3 must come from somewhere. The source of the oxygen becomes an interesting issue if the gray hematite deposits are truly ancient, which would mean that volcanism was continuously active preventing significant concentrations of atmospheric O_2 because of the input of reducing gases (see below), and if the hematite deposits are tens of meters thick, which would mean a considerable oxygen inventory. For example, if the $\sim 175{,}000$ km^2 of hematite in Sinus Meridiani is 10 m thick, and comprises $\sim 20\%$ hematite, then we have

$$[0.2 \times (1.75 \times 10^{11} \text{ m}^2) \times (10 \text{ m})$$
$$\times (5275 \text{ kg Fe}_2\text{O}_3 \text{ m}^{-3})]/(0.1597 \text{ kg Fe}_2\text{O}_3 \text{ mol}^{-1})$$
$$= 1.16 \times 10^{16} \text{ moles}$$

of hematite. This requires 5.8×10^{15} moles of O_2, given that 1 mole of O_2 produces 2 moles of hematite: $4FeO + O_2 = 2Fe_2O_3$. This is a significant amount of oxygen, more than 6 times the total amount of free O_2 present in today's martian atmosphere ($\sim 9.6 \times 10^{14}$ moles O_2). The Meridiani Formation is special because it has been exposed geologically recently, perhaps in the last ~ 10 myr on the basis of crater counts (Hartmann et al., 2001). If there are other buried layers of gray hematite, perhaps some of the meter-scale layers visible in MOC images in the walls of craters and canyons, that are inaccessible to TES spectral mapping, then the Meridiani hematite and the smaller deposits elsewhere could be only a tiny fraction of the total gray hematite produced on early Mars. As noted above, light-toned caprock is likely to hide underlying hematite in Aram Chaos. There could also have been gray hematite deposits that were exposed in the last 4 byr of martian history but have disappeared due to wind erosion and the transformation of gray hematite to finely divided red-colored oxides. For example, if the Meridiani Formation represents only 1/10th of a total inventory (perhaps because the rest is buried or has been stripped away), we would require the equivalent of ~ 60 times the amount of O_2 in the present martian atmosphere to have been available on early Mars. Again, this estimate assumes a 10-m scale thickness for the extant deposit, which seems reasonable on the basis of layered geomorphology (see Sections 5 and 6), but could be an overestimate. The main point is that the amount of oxygen required to make hematite is clearly relevant to the questions of

(1) whether the hematite originated from iron oxides produced in a standing body of water from atmospheric oxidation and was subsequently recrystallized to coarse-grained form, or
(2) whether the gray hematite was the direct result of hydrothermal activity.

We suggest that the oxygen balance probably favors the latter hypothesis, as we now consider.

7.2. Oxygen in the atmosphere of early Mars

Is vast oxidation of the iron in a standing a body of water on early Mars plausible? If anything, the early martian atmosphere would have been much more anoxic than the present atmosphere because of the continuous flux of oxygen-consuming reduced volcanic gases. Volcanic gases never contain free oxygen and instead always contain reducing gases (H_2, CO, SO_2, and H_2S) that react with any oxygen in the atmosphere to remove it (e.g., Holland, 1984). Because the rate of oxidation of aqueous iron is sensitive to O_2 levels, then it is useful to estimate what the O_2 levels might have been and then to estimate oxidation rates. We can roughly estimate the concentration of O_2 in the early martian atmosphere following the method suggested by Walker (1978) for estimating the prebiological concentration of oxygen in the Earth's atmosphere. In the hydrogen budget of the early martian atmosphere, volcanism would release H_2 into the atmosphere and H_2 would accumulate to a level where the input flux was balanced by losses. Hydrogen sinks include direct escape to space and rapid photochemical reaction with net oxygen produced from water vapor destruction. Here, net oxygen is that derived from water molecules that were photolyzed followed by hydrogen escape. A markedly higher concentration of CO_2 on early Mars, which may or may not have been the case (e.g., Kasting, 1991; Forget and Pierrehumbert, 1997), does not significantly affect the hydrogen balance considered here. Thus, we have

$$F_{\text{volcanic}} = F_{\text{H-escape}} + F_{\text{net-O}_2}, \tag{5}$$

where F_{volcanic} is the volcanic flux of H_2 that balances both the direct escape of hydrogen to space ($F_{\text{H-escape}}$) and the reaction of hydrogen with oxygen produced from net destruction of H_2O molecules ($F_{\text{net-O}_2}$). Of course, we should also consider other reduced volcanic gases that photochemically react with oxygen such as CO. But from the standpoint of overall redox balance, it is reasonable to think of these other reduced gases as effective fluxes of hydrogen and lump them all together. For example, the net photochemical oxidation of CO can be thought of as a source of H_2 via $CO + H_2O = CO_2 + H_2$, and similar relationships hold for other reduced volcanic gases such as H_2S and SO_2. By considering only H_2, we are merely being generous for the survival of oxygen in order to estimate an upper limit. As shown by Hunten (1973) and Walker (1977), the rate of net water vapor destruction (and generation of oxygen) depends on the rate of escape of hydrogen and is controlled by the slow upward transport of hydrogen through the atmosphere to the exosphere. Under quite general conditions, this upward transport is limited by diffusion through the thermosphere. In the diffusion-limited approximation, the escape rate for hydrogen from H_2 molecules and from photolyzed water is proportional to their mixing ratios in the lower atmosphere of Mars above the cold-trapping level for H_2O. Consequently, the rate of escape of hydrogen can be written as $F_{\text{H-escape}} = k_e f_{H_2}$, where f_{H_2} is the

Table 1
A much simplified model for the redox balance in the early martian atmosphere

Reaction #	Reaction	Rate constant	Reference/Note
		Hydrogen and water photochemistry	
R1	$H_2O + h\upsilon = OH + H$	$R \sim 1.1 \times 10^{12}$ cm^{-2} sec^{-1}	Integrated through the lower atmosphere
R2	$OH + H_2 = H_2O + H$	$K_1 = 5.5 \times 10^{-12} \exp(-2000/T)$ cm^3 s^{-1}	DeMore et al. (1992)
R3	$H + H + M = H_2 + M$	$K_2 = 1.5 \times 10^{-29} T^{-1.3}$ cm^6 s^{-1}	Tsang & Hampson (1986)
		Photochemistry that destroys oxygen	
R4	$H + O_2 + M = HO_2 + M$	$K_3 = 5.7 \times 10^{-32} (300/T)^{-1.6}$ cm^6 s^{-1}	DeMore et al. (1992)
R5	$HO_2 + H = OH + OH$		
R6	$2OH + 2H_2 = 2H_2O + 2H$		
R4 + R5 + R6	Net reaction: $2H_2 + O_2 = 2H_2O$		

The table shows the photochemical steps leading to mutual photochemical annihilation of oxygen and hydrogen in the early martian atmosphere. "M" designates an arbitrary third molecule, most probably CO_2 or N_2. Temperature-dependent rate constants are listed for the essential reactions that control the atmospheric abundance of hydrogen and of oxygen, where T is in K.

hydrogen volume mixing ratio in the lower atmosphere and k_e is a constant ($\approx (1.1–2.5) \times 10^{13}$ cm^{-2} s^{-1}, depending on the assumed CO_2 versus N_2 composition of the atmosphere of early Mars) (Walker, 1977). Similarly, $F_{net-O_2} = k_e f_{H_2O}$, where f_{H_2O} is the water vapor volume mixing ratio. Thus Eq. (1) can be re-written as

$$f_{H_2} = \frac{F_{volcanic} - k_e f_{H_2O}}{k_e}. \qquad (6)$$

Here f_{H_2O} can be estimated by using the equilibrium vapor concentration at an estimated temperature for the early martian tropopause. The volcanic flux of hydrogen on early Mars, $F_{volcanic}$, can also be estimated. The total rate of release of volcanic gases, including hydrogen, was greater on early Mars than today because of larger rates of internal heating due to the decay of radioactive elements. However, volcanic outgassing on Mars was still much less than on Earth: Jakosky and Shock (1998) estimated a factor of ~ 250 times less than Earth (see their Fig. 1), which we adopt here. Today, the terrestrial volcanic flux of H_2 is estimated as $(1.8 \pm 1.4) \times 10^{10}$ H_2 molecules cm^{-2} s^{-1} (Holland, 2002). At about 4.0 Ga, the heat flux from the Earth was 2–4 times greater, so the volcanic flux would be greater, roughly scaling with the square of the heat flux (Schubert et al., 2001). Let us take the early volcanic flux as ~ 4 times greater at 4 Ga. If the early martian flux had been 250 times less than early Earth's flux, then the globally averaged volcanic flux of H_2 on early Mars was $F_{volcanic} \sim 3.6 \times 10^8$ H_2 molecules cm^{-2} s^{-1}. If the martian mantle had been more reducing than Earth's, as suggested by Wadhwa's (2001) martian meteorite data, then the proportion of reduced gases from volcanic emissions would have been much greater, leading to a significantly higher H_2 flux. However, Wänke and Dreibus (1994) present geochemical arguments that the martian mantle was oxidized early, so we stay with the conservative assumption that the redox partitioning of martian volcanic gases was buffered in favor of only a weakly reducing mixture, much like modern terrestrial volcanic gases (Holland, 1984). If we take a water mixing ratio similar to Earth's tropopause ~ 4 ppmv as being similar to that in the tropopause of a wet early Mars

(corresponding to a temperature of about 195 K), then solving Eq. (6) gives $\sim 10^{-5}$ or ~ 10 ppmv for the mixing ratio of H_2 on early Mars. This is roughly similar to the H_2 mixing ratio in the martian atmosphere today (Krasnopolsky and Feldman, 2001), but the situation differs because in our scenario a flux of H_2 is being continuously consumed by O_2 and replenished by volcanism to maintain the equilibrium H_2 mixing ratio in the atmosphere.

To estimate the concentration of O_2 requires some consideration of photochemistry. To provide an upper limit on O_2, we make the generous assumption that all of the O_2 produced by the photodissociation of water on early Mars got transported to the lower atmosphere. The photochemical reactions that destroy O_2 are summarized in Table 1. From the equations in Table 1, the concentration of O_2 is given by

$$[O_2] = \frac{\text{net-}O_2 \text{ source (molecules cm}^{-2}\text{ s}^{-1})}{k_3[H][M] \times H_s} \qquad (7)$$

and the hydrogen atom concentration is given by

$$[H]^2 = \frac{2R}{k_2[M] \times H_s}. \qquad (8)$$

Here R is the height-integrated rate of photolysis of tropospheric water vapor in cm^{-2} s^{-1}. Consequently, the expressions include the atmospheric scale height, H_s, because, for example, the height-integrated rate of destruction of O_2 is $k_3[O_2][H][M] \times H_s$, considering reaction R4 in Table 1. To estimate R, we can take the globally averaged photon flux between 184–200 nm and generously assume (for O_2 production) that this is all used in the photolysis of water vapor. This gives $R = 1.1 \times 10^{19}$ cm^{-2} s^{-1} at the distance of Mars. (We do not consider the spectral region below ~ 184 nm because absorption by CO_2 dominates at such wavelengths and shields water vapor in the lower atmosphere from short ultraviolet wavelengths (e.g., Cockell et al., 2000). The concentrations from Eqs. (7) and (8) are sensitive to the assumed total atmospheric density at the ground, [M], which would be 2.6×10^{19} molecules cm^{-3} for a thick early Mars atmosphere at 1 bar, but otherwise scales with surface pressure. Assuming a tropospheric temperature, we can solve (7) and (8) for [O_2] and deduce the oxygen partial pressure

(pO$_2$). For surface pressures of 10 mbar to 1 bar, pO$_2$ varies from $\sim 10^{-12}$ to $\sim 10^{-15}$ bar. Neither the assumed tropospheric temperature nor the assumed scale height makes much difference to the order of magnitude of the result within the realm of reasonable possibilities (cold-trap temperatures of 160–300 K and atmospheric scale heights of 5–15 km). Of course, in reality, minor species like O$_2$ would not be distributed uniformly with height so that Eqs. (7) and (8) are only rough approximations. But the point of this calculation is to show that the pO$_2$ would be far smaller than today's pO$_2$ on Mars, $\sim 7.8 \times 10^{-6}$ bar. This result arises simply because in the early martian atmosphere there would be a small volcanic flux of H$_2$ (and other reduced gases) to consume O$_2$, unlike the case today, where the volcanic flux is negligible. Moreover, the volcanic flux of H$_2$ would have significantly exceeded the net production flux of O$_2$ arising from net water vapor destruction, forcing the dynamic equilibrium concentration of O$_2$ to low values.

7.3. Iron oxidation rates

Now that we have an estimate of pO$_2$ on early Mars, we can consider the oxidation rates of aqueous iron on early Mars. Our purpose here is to examine the hypothesis that oxidation of ferrous iron in a large standing body of water led to the original iron oxide sediments that were later transformed to crystalline hematite: one of the suggestions of Christensen et al. (2000). Burns (1993) describes the oxidation rate of ferrous iron

$$\frac{d[Fe^{2+}]}{dt} = -k_B[Fe^{2+}][O_2]\{OH^-\}^2 \tag{9}$$

where [Fe^{2+}] is the molar concentration of ferrous iron, [O$_2$] is the molal concentration of oxygen, and $\{OH^-\}$ is the activity of OH$^-$. The constant, k_B, in mol^{-3} min^{-1}, depends on the temperature (T) and ionic strength (I) of the solution as follows: $k_B = 21.56 - 1545/T + AI^{0.5} + BI^{0.5}/T + CI$, where A, B, and C are constants tabulated by Burns (1993). The hydroxyl $\{OH^-\}$ is a direct function of the pH of the solution, because pH $= -\log_{10}\{H^+\}$, by definition, and $\{H^+\}\{OH^-\} = K_w =$ the dissociation constant for liquid water. Thus, if one specifies the pH, oxygen concentration, and ionic strength of an aqueous solution, the rate of oxidation can be calculated. By considering the density of hematite and deposition over a unit area, the depth of hematite that is produced per unit time can also be calculated. Figure 8 shows such a calculation, where pO$_2$ has been varied from today's martian value ($\sim 10^{-5}$ bar) to a value expected on a volcanically active early Mars ($\sim 10^{-12}$ bar), as calculated above. The aqueous solution is assumed to be brine, arbitrarily 1 molal ionic strength (compared to 0.7 molal for terrestrial seawater) at 0 °C. The ferrous iron concentration is assumed to be 5 mg l^{-1}, which is a reasonable rough estimate for an iron-rich fluid. One can compare the Precambrian deep ocean, which is estimated to have contained ~ 3 mg Fe^{2+} l^{-1} (Holland, 1984). We have not included
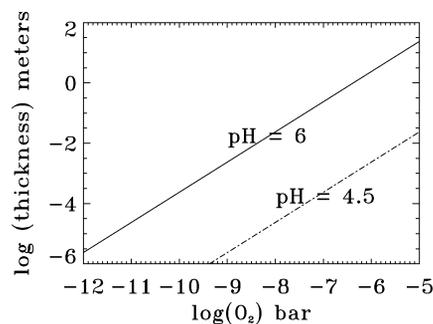
Fig. 8. The thickness of hematite in meters (at the density of crystalline hematite) that could be produced from a standing body of water over a million Earth years for solutions at pH ~ 4.5–6.0 and various fixed oxygen levels in the atmosphere. A ferrous iron loading of 5 mg l^{-1} is assumed for the solution (see text).

higher pH levels in Fig. 8, because natural waters of pH > 7 contain hardly any dissolved iron. Typically only acid solutions are capable of holding significant amounts of dissolved iron. For example, in the eastern province of Kamchatka, Russia, acid rivers with pH $= 4.5$–5.3 contain 1–7.8 mg l^{-1} of iron due to leaching of ashy volcanic material. Highly acid hydrothermal waters with pH $= 0$–3, such as the hot springs of the Ebeko volcano on the Kuril archipelago, Russia, contain up to 100–300 mg l^{-1} of dissolved iron (Melnik, 1982, pp. 145–151). Figure 8 shows that very little hematite could be produced in a standing body of water on early Mars with a low atmospheric pO$_2$ of $\sim 10^{-12}$ bar. If a lake with a pH of 6 stood for 10 myr it would only produce a paltry 10 μ thick deposit. This compares to the annual iron oxide precipitation in the Hamersley BIF in Australia, reported as ~ 20–100 m Myr^{-1} (Trendall and Blockley, 1970, p. 336) and 100–1000 m Myr^{-1} (Barley et al., 1997). One alternative to this scenario is that the iron oxide formed later in martian history when volcanism was merely episodic and pO$_2$ was similar to today's value $\sim 10^{-5}$ bar. However, climatic conditions have probably not been conducive to large bodies of standing water on the surface in post-Noachian times given very low post-Noachian erosion rates, which are more likely explained by wind. A more plausible alternative is that oxidation may have been produced hydrothermally by the dissociation of water and loss of hydrogen. The evolution of hydrogen that is required by redox balance is confirmed in laboratory experiments when hematite is produced hydrothermally (e.g., Kolb et al. (1973) report evolution of H$_2$). Thus the redox balance on early Mars favors the hydrothermal hypothesis for the formation of gray hematite. Another alternative pathway for forming iron oxides is photo-oxidation in standing bodies of water, which we consider below, although this would again require burial metamorphism and hydrothermal alteration to effect a recrystallization to gray hematite.

7.4. Photo-oxidation alternative?

In Section 3.2, we discussed the hypothesis that BIFs on Archean Earth may have been abiotically produced by

photo-oxidation (Braterman et al., 1983). Although this hypothesis is unlikely to have been correct for early Earth for the several reasons we gave, the possibility remains that waters on early Mars may have been more conducive to photo-oxidation. This would require that the fluids somehow contained plenty of dissolved iron but very little dissolved silica. In idealized theory, the photo-oxidation mechanism is capable of producing a relatively high rate of oxidation and deposition despite the factor of 2.3 times less solar radiation on Mars than on Earth. Given the quantum efficiency from laboratory studies, assuming 50% cloud cover, and assuming an integrated column of 10 m water we can estimate the photo-oxidation rate (Braterman et al., 1983; Anbar and Holland, 1992). Ignoring light loss (reflection, scattering) in the water column, one calculates ~ 40–200 m Fe_2O_3 per 10^6 yr, which is in the right ballpark to account for observations. Here the conversion of iron oxides to coarsely crystalline variety by subsequent thermal processing is presumed. The photo-oxidation would liberate substantial H_2. For example, if the hematite areas that we see on Mars were all generated at the same time, the rate of H_2 production would be roughly $\sim 5 \times 10^{10}$ H_2 molecules $cm^{-2}\,s^{-1}$ as a global average. This rate would cause H_2 to accumulate in the atmosphere to a significant mixing ratio of $\sim 10^{-3}$, assuming diffusion-limited escape, which has potential implications for biology mentioned below.

8. Biological implications for the environment on early Mars?

8.1. Could there have been biological oxidation on early Mars?

In this paper, we have noted that there are several means to form gray, crystalline hematite on Mars but that the geology and topography of Aram Chaos, when combined with consideration of redox chemistry, suggest that hydrothermal activity is the mechanism that would require the least special circumstances. However, it is worth considering whether biology could have been involved given the inherent importance of such an inference. All life thrives via redox chemistry and thus life will inevitably leave a large redox imprint on its surroundings: witness Earth's O_2-rich atmosphere and ocean. If there had been a global biota on early Mars, its most obvious (i.e., large-scale) manifestation would undoubtedly be the geochemical remains of large redox anomalies. Several mechanisms could oxidize ferrous iron and all of these stoichiometrically require oxygen as described above. There are only two possibilities for an oxygen source:

(1) Oxygen was abiotically produced from water as hydrogen escaped to space and ferrous iron acted as a sink for this oxygen.
(2) Alternatively, early Mars, like early Earth, had a microbial biosphere that either liberated oxygen by oxygenic

photosynthesis or catalyzed the oxidation of ferrous iron with CO_2.

There are at least two reasons why the idea of oxygen-producing microbes would be consistent with the controversial belief that magnetite crystals of biogenic shape in ALH84001 represent the remains of magnetotactic bacteria (McKay et al., 1996; Kirschvink et al., 2002; Barber and Scott, 2002). First, magnetotactic bacteria use the magnetic properties of magnetite to guide themselves along a redox gradient away from a surface environment dominated by oxygen to an oxic-anoxic boundary where both oxidant and reductant are available for the metabolic release of energy. Second, magnetotactic bacteria metabolize either O_2 or sulfate, where the latter must ultimately derive from the net oxygen source of hydrogen escape. Another possible (but speculative) line of evidence in favor of biological oxygen production on early Mars is the presence of 3.9 Ga carbonates in the ALH84001 meteorite that are enriched in ^{17}O relative to the oxygen isotope composition of martian bulk silicates. Mass balance requires that there must be a significant oxygen reservoir depleted in ^{17}O relative to martian bulk silicates to account for the ^{17}O-enriched carbonates. Farquhar et al. (1998) have suggested that the enrichment of ^{17}O in carbonates was derived from mass-independent photochemical reactions in the atmosphere that imparted a ^{17}O-enrichment to CO_2. However, they note that the mass balance cannot be explained away by ^{17}O-depleted O_2 in the present atmosphere because the quantity of O_2 is far too small and much oxygen must be in the crust. Farquhar's interpretation that fractionation is induced by tropospheric chemistry has recently been challenged, although their overall mass balance must still apply. Classical kinetic isotope fractionation during the respiration of O_2 causes a similar "mass independent" oxygen isotope fractionation in the Earth's troposphere (Young et al., 2002). If O_2 had been produced biologically on early Mars, we would expect analogous fractionation due to microbial respiration. This is potentially testable. O isotopes in hematite on Mars should be depleted in ^{17}O if they had a contribution from biological O_2, noting that the signature may be somewhat weakened by subsequent hydrothermal recrystallization and exchange with water. In contrast, if the hematite originated solely from abiotic hydrothermal dissociation of water, the oxygen isotope composition should be similar to bulk silicates given that hot water should be close to isotopic equilibrium with the host rock. Of course, if the case for biology turns out to be true, we would necessarily conclude that Mars is red because of life (a possibility first suggested by Hartman and McKay, 1995), in the same way that Earth developed continental red beds at ~ 2.3 Ga solely in response to the action of an oxygen-producing biosphere (Holland, 1984). In this case, merely to view Mars with the naked eye and to see its color would be to detect signs of ancient life, which would be a curious conclusion from our elaborate space exploration efforts.

8.2. The relevance of Fe^{3+} for primitive life

In a less speculative scenario, hematite was most likely produced by abiotic hydrothermal activity, accompanied by the evolution of hydrogen and its loss to space. However, even this abiotic scenario would produce favorable environmental conditions for primitive life, potentially enabling it to thrive if it ever got started. The most significant biochemical implication of hematite concentrations on Mars is that ferric iron was being generated in an environment where liquid water and reductant (H_2) were also readily available. H_2 itself is not particularly special: it is certain to have been produced by volcanism on early Mars. But Fe^{3+} (an electron acceptor) should have been very scarce on the early planet. As emphasized by Russell and Hall (1999), Fe^{3+} and H_2 make an excellent redox couple for the most primitive form of life without any complicated enzymes. Also, in the case of a photo-oxidation source of ferric iron, H_2 would be generated at a rate sufficient to induce an atmospheric H_2 mixing ratio $\sim 10^{-3}$, which would be biologically significant. At this concentration, primitive methane-producing microbes are able to draw CO_2 and H_2 directly from the air and use them as a redox couple for the metabolic process $4H_2 + CO_2 = CH_4 + 2H_2O$ (Kral et al., 1998), thereby creating a significant greenhouse gas. These thoughts, of course, are highly speculative, but the paucity of our present certainties about Mars does not preclude them. They are worth mentioning in the context of future exploration efforts that are concerned with the question whether there was life on early Mars.

9. Conclusions

9.1. A hydrothermal origin for gray hematite

We conclude that the gray crystalline hematite in Aram Chaos most likely resulted from hydrothermal activity. This deduction is based on the combination of three pieces of information:

(1) Thermal processing at temperatures $\gtrsim 100\,^{\circ}C$ is necessary to produce gray crystalline hematite based on thermodynamic calculations and bearing in mind the warm temperature constraint associated with all known occurrences of gray crystalline hematite on Earth. We specify a lower limit temperature of roughly $100\,^{\circ}C$ based on a combination of laboratory studies, field studies, and theoretical calculations (Sections 3.2, 3.3, and 4).

(2) The chaotic, jumbled terrain of Aram Chaos is thought to have formed by the geothermal melting of ground ice or the expulsion of groundwater, causing a loss of support and collapse of overlying material (Sharp, 1973). Fissuring and volcanism likely initiated the formation of the chaotic terrain. Such a geological context would

have been accompanied and probably preceded by hydrothermal activity.

(3) The topography of the gray hematite region in Aram Chaos indicates its occurrence in geologic strata restricted in vertical extent, i.e., within a specific topographic range. This is consistent with an ancient aquifer, which at one point, we postulate, was hydrothermally charged.

All of the above are consistent with a hydrothermal origin for the gray hematite. An ancillary piece of information is that the aerial oxidation of large areas of basalt or iron dissolved in solution to form hematite seems unlikely to have been facilitated on early Mars by a sufficiently oxidizing atmosphere (Section 7) unless there was the extraordinary circumstance of a biological source (Section 8). In contrast, hydrothermal oxidation is a mechanism that seems almost certain for early Mars given the presence of geothermal heat along with subsurface water or ice. Our view concerning the hydrothermal formation of hematite in Aram Chaos is supported by analogs on Earth, such as the formation of massive specularite by hydrothermal activity and metasomatism in ancient rocks in Yukon, Canada, that were brecciated by forceful release of hydrothermal fluids (Thorkelson et al., 2001).

We cannot entirely rule out the alternative possibility that the martian hematite originated as iron oxide beds in sedimentary deposition from a lake or sea and that the iron oxides were subsequently recrystallized to gray hematite by burial metamorphism (e.g., Lane et al., 2002b), akin to terrestrial BIFs. However, even if this were the case, recent analysis of terrestrial BIF hematite ore deposits suggests an important role for hydrothermal activity and metasomatism during burial metamorphism for the recrystallization of iron oxides like magnetite or goethite into coarsely crystalline hematite (Barley et al., 1999; Taylor et al., 2001). Thus hydrothermal activity and burial metamorphism are not mutually exclusive for forming coarsely crystalline hematite; there is a gray area of overlap, so to speak. The strongest evidence in favor of a sedimentary origin on Mars is that the hematite deposits are clearly associated with layered geomorphology in all cases, the Meridiani Formation, Vallis Marineris, and Aram Chaos (Christensen et al., 2001). On the other hand, such layering is ubiquitous throughout the ancient terrain on Mars (Malin and Edgett, 2000), whereas exposures of gray hematite are rare. An alternative relationship is that suitable layering may be necessary to provide an impermeable cap to trap a hydrothermal aquifer. The relatively smooth texture of the caprock immediately superjacent to the hematite-bearing outcrops in Aram Chaos (Figs. 5–7) may be a consequence of the caprock immediately above the hematite rock being mechanically homogeneous and perhaps massive and relatively impermeable. The erosional pitting and etching of the hematite-bearing outcrops could be the consequence of a form of cavernous weathering, in which fluids passing though such rock dif-

ferentially cement (or uncement) the rock. Subsurface flow within Aram Chaos is implicit in the formation of the chaos (e.g., Sharp, 1973; Carr, 1979). On the Earth, fluids passing through permeable rock often evolve into elaborate maze-like flow systems (e.g., Dunne, 1990). These flow networks can occur on decameter scales. Once exposed to wind abrasion, this differential cementing would express itself as decameter scale differential erosion, as seen on some strata in Aram Chaos.

Lane et al. (2000, 2001, 2002a, 2002b) favor a sedimentary, schistose origin to create the necessary physical conditions to form specular hematite, although they also suggest hydrothermal mechanisms. Platy crystals can grow when deposited from a hydrothermal solution or grown under metasomatic conditions. As demonstrated by Martin and Piwinskii (1969), formation of specularite can even result from hydrothermal vapor deposition, an environment far removed from lacustrine sedimentation. Hydrothermal activity can also explain the apparent absence of large amounts of other minerals, such as silica, associated with acid weathering of basalt. Iron oxide is very much less soluble and more dense than silica. Silica solubility increases significantly with temperature (and to a much lesser degree with pressure), so any silica associated with the formation of hematite could be leached away in hydrothermal solution, while highly insoluble, dense and immobile hematite would remain. Silica solubility is approximately given by (Wollast, 1974)

$$\log(\text{molality amorphous silica}) = -0.309 - 0.723 \left(10^3/T\right)$$

where T is in Kelvin. ("Molality" is simply the moles of solute (SiO_2) per kg of water.) Using this equation, silica solubility, by mass, is about 66 ppm at $0\,^{\circ}C$, increases to 340 ppm at $100\,^{\circ}C$, and reaches $\sim 0.4\%$ at $600\,^{\circ}C$. In the case of Aram Chaos, silica could have dissolved and flowed out of Aram Chaos where it would be dispersed detritally at low relative abundance.

9.2. Implications for future observations of the gray hematite

Given that hydrothermal activity seems the most likely explanation for forming the hematite in Aram Chaos, parsimony would dictate that it was the mechanism that produced the other hematite deposits in Vallis Marineris and Sinus Meridiani. In the latter case, this would suggest very extensive hydrothermal systems on early Mars. The Mars Exploration Rover (MER) mission, launched in 2003, will be able to study iron minerals given that each rover payload includes a mini-TES, Mössbauer spectrometer, alpha–proton spectrometer, microscopic imager, and rock abrasion tool. The following investigations of the gray hematite by MER and other future missions may help elucidate its origin:

- Hematite could show signs indicative of hydrothermal activity such as hydrothermal minerals that are at a sufficiently low abundance that they are not detectable

by TES on MGS. In Sinus Meridiani they may be detectable by mini-TES.

- A close-up view of the gray hematite crystals on Mars (e.g., with a microscopic imager or other camera) will help distinguish petrological features such as bedding, veining, or matrix structure. Veins, fracture fillings, and clast or wall coatings provide common evidence of fluid motion. We expect such features on Mars if the origin of the gray hematite is hydrothermal. This could be important if we see little evidence of hydrothermal accessory minerals. For example, veins of pure specularite are found in basalt in some of the oldest terrestrial rocks in Isua, Greenland, with an apparent hydrothermal origin but no significant abundance of accompanying ancillary minerals (R. Buick, private communication). Presumably, large amounts of hydrothermal fluid were responsible for removing all but the most highly insoluble and poorly transported dense mineral, namely hematite. It is possible that an analogous predicament could exist on Mars.
- We expect hydrothermal hematite to be low in Al, Ti, and trace elements associated with sedimentary processes.
- Magnetic studies may help constrain an upper limit on the temperature that the hematite experienced. The Curie point (of magnetic disordering) is $\sim 680\,^{\circ}C$.
- Oxygen isotopes in the hematite and any accompanying minerals may also set some constraints on the temperature and mode of formation.
- A study of triple oxygen isotope system (^{18}O, ^{17}O, and ^{16}O), in particular, may provide clues about whether or not there was any biological influence in the oxidation process of ferrous iron. We expect the hematite to have ^{17}O-depleted oxygen if it resulted from the influence of a significant biosphere on early Mars. This expectation is tempered, however, by the realization that if precursor fine-grained iron oxides were produced under biological influence, hydrothermal activity necessary for hematite recrystallization would likely reset the oxygen isotope composition.

In summary, sophisticated isotopic and trace mineral analysis would be necessary to better understand the origin of the hematite. Consequently, there is good reason to try to include gray hematite samples with returned samples from Mars in the future.

References

Anbar, A.D., Holland, H.D., 1992. The photochemistry of manganese and the origin of banded iron formations. Geochim. Cosmochim. Acta 56, 2595–2603.

Allen, C.C., Westall, F., Schelble, R.T., 2001. The importance of the martian hematite site for astrobiology. Astrobiology 1, 111–123.

Baird, A.K., Clark, B.C., 1981. On the original igneous source of martian fines. Icarus 45, 113–123.

Banin, A., Clark, B.C., Wänke, H., 1992. Surface chemistry and mineralogy. In: Kieffer, H.H., et al. (Eds.), Mars. Univ. of Arizona Press, Tucson, pp. 594–625.

Barber, D.J., Scott, E.R.D., 2002. Origin of supposedly biogenic magnetite in the martian meteorite Allan Hills 84001. Proc. Nat. Acad. Sci. 99, 6556–6561.

Barley, M.E., Pickard, A.L., Sylvester, P.J., 1997. Emplacement of a large igneous province as a possible cause of banded iron formation 2.45 billion years ago. Nature 385, 55–58.

Barley, M.E., Pickard, A.L., Hagemann, S.G., Folkert, S.L., 1999. Hydrothermal origin for the 2 billion year old Mount Tom Price giant iron ore deposit, Hamersley province, Western Australia. Miner. Deposita 34, 784–789.

Barnes, H.L., 1979. Solubilities of ore minerals. In: Barnes, H.L. (Ed.), Geochemistry of Hydrothermal Ore Deposits. Wiley, New York, pp. 404–460.

Becker, B.H., Clayton, R.N., 1976. Oxygen isotope study of a Precambrian banded iron formation, Hamersley Range, Western Australia. Geochim. Cosmochim. Acta 40, 1153–1165.

Best, M.G., 1982. Igneous and Metamorphic Petrology. Freeman, San Francisco.

Beukes, N.J., Klein, C., 1992. Models for iron-formation deposition. In: Schopf, J.W., Klein, C. (Eds.), The Proterozoic Biosphere. Cambridge Univ. Press, New York, pp. 147–152.

Bischoff, J.L., 1969. Goethite–hematite stability relations with relevance to sea water and the Red Sea brine system. In: Degens, E.T., Ross, D.A. (Eds.), Hot Brines and Recent Heavy Metal Deposits in the Red Sea. Springer-Verlag, New York, pp. 402–406.

Blatter, D.L., Carmichael, S.E., 1998. Hornblende peridotite xenoliths from central Mexico reveal the highly oxidized nature of subarc upper mantle. Geology 26, 1035–1038.

Bookstrom, A.A., 1995. Magmatic features of iron-ores of the Kiruna type in Chile and Sweden—-ore textures and magnetite geochemistry—a discussion. Econ. Geol. 90, 469–473.

Bouska, V., Bell, J.F., 1993. Assumptions about the presence of natural glasses on Mars. J. Geophys. Res. 98, 18719–18725.

Braterman, P.S., Cairns-Smith, A.G., Sloper, R.W., 1983. Photo-oxidation of hydrated Fe^{2+}-significance for banded iron formations. Nature 202, 163–164.

Brocks, J.J., Logan, G.A., Buick, R., Summons, R.E., 1999. Archean molecular fossils and the early rise of eukaryotes. Science 285, 1033–1036.

Broman, C., Nyström, J.O., Henríquez, F., Elfman, M., 1999. Fluid inclusions in magnetite–apatite ore from a cooling magmatic system at El Laco, Chile. GFF 121, 253–267.

Burns, R.G., 1993. Rates and mechanisms of chemical weathering of ferromagnesian silicate materials on Mars. Geochim. Cosmochim. Acta 57, 4555–4574.

Calvin, W.M., 1998. Could Mars be dark and altered? Geophys. Res. Lett. 25, 1597–1600.

Carr, M.C., 1979. Formation of martian flood features by release of water from confined aquifers. J Geophys. Res. 84, 2995–3007.

Catling, D.C., 1999. A chemical model for evaporites on early Mars: possible sedimentary tracers of the early climate and implications for exploration. J. Geophys. Res. 104, 16453–16470.

Chapman, M.G., Tanake, K.L., 2002. Related magma–ice interactions: possible origins of Chasmata, Chaos, and surface materials in Xanthe, Margaritifer, and Meridiani Terae, Mars. Icarus 55, 324–339.

Chaudhuri, A., 1967. On the occurrence of specularite. Quart. J. Geol. Mining Metallurg. Soc. India 29, 53–54.

Christensen, P.R., Morris, R.V., Lane, M.D., Bandfield, J.L., Malin, M.C., 2001. Global mapping of martian hematite mineral deposits: remnants of water-driven processes on early Mars. J. Geophys. Res. 106, 23873–23885.

Christensen, P.R., Bandfield, J.L., Clark, R.N., Edgett, K.S., Hamilton, V.E., Hoefen, T., Kieffer, H.H., Kuzmin, R.O., Lane, M.D., Malin, M.C., Morris, R.V., Pearl, J.C., Pearson, R., Roush, T.L., Ruff, S.W., Smith, M.D., 2000. Detection of crystalline hematite mineralization on Mars by the Thermal Emission Spectrometer: evidence for near-surface water. J. Geophys. Res. 105, 9623–9642.

Clifford, S.M., 1993. A model for the hydrologic and climatic behavior of water on Mars. J. Geophys. Res. 98, 10973–11016.

Cloud, P., 1973. Paleoecological significance of the banded iron-formation. Econ. Geol. 68, 1135–1143.

Cloud, P., 1988. Oasis in Space. Norton, New York.

Cockell, C.S., Catling, D.C., Davis, W.L., Snook, K., Kepner, R.L., Lee, P., McKay, C.P., 2000. The ultraviolet environment of Mars: biological implications past, present, and future. Icarus 146, 343–459.

Cornell, R.M., Schwertmann, U., 1996. The Iron Oxides. VCH Publishers, New York.

Crerar, D., Scott, W., Brantley, S., 1985. Chemical controls on solubility of ore-forming minerals in hydrothermal solutions. Can. Mineral. 23, 333–352.

De Boer, C.B., Mullender, T.A.T., Dekkers, M.J., 2001. Low-temperature behaviour of hematite: susceptibility and magnetization increase on cycling through the Morin transition. Geophys. J. Int. 146, 201–216.

Delano, J.W., 2001. Redox history of the Earth's interior since 3900 Ma: implications for prebiotic molecules. Origins Life Evol. B. 31, 311–341.

DeMore, W.B., Golden, D.M., Hampson, R.F., Howard, C.J., Kurylo, M.J., Molina, M.J., Ravishankara, A.R., Sander, S.P., 1992. Chemical kinetics and photochemical data for use in stratospheric modeling. Eval. No. 10, JPL Publication 92-20. Jet Propulsion Laboratory, Pasadena.

Des Marais, D., 1994. The Archean atmosphere: its composition and fate. In: Condie, K.C. (Ed.), Archean Crustal Evolution. Elsevier, New York, pp. 505–523.

Diakonov, I., Khondakovsky, I., Schott, J., Sergeeva, E., 1994. Thermodynamic properties of iron oxides and hydroxides. I. Surface and bulk thermodynamic properties of goethite (α-FeOOH) up to 500 K. Eur. J. Mineral. 6, 967–983.

Diamandescu, L., Mihaila-Tarabasanu, D., Popescu-Pogrion, N., Totovina, A., Bibicu, I., 1999. Hydrothermal synthesis and characterization of some polycrystalline α-iron oxides. Ceram. Int. 25, 689–692.

Dunne, T., 1990. Hydrology, mechanics, and geomorphic implications of erosion by subsurface flow. In: Higgins, C.G., Coates, D.R. (Eds.), Groundwater Geomorphology; The Role of Subsurface Processes and Landforms. In: Geological Society of America Special Paper, Vol. 252. Boulder, pp. 1–28.

Edgett, K.S., Parker, T.J., 1997. Water on early Mars: possible subaqueous sedimentary deposits covering ancient cratered terrain in western Arabia and Sinus Meridiani. Geophys. Res. Lett. 24, 2897–2900.

Edgett, K.S., Malin, M.C., 2000a. Examples of martian sandstone: indurated, lithified, and cratered eolian dunes in MGS images. In: Proc. Lunar Planet. Sci. Conf. 31st. #1071 (abstract).

Edgett, K.S., Malin, M.C., 2000b. The new Mars of MGS MOC: ridged layered geologic units (they're not dunes). In: Proc. Lunar Planet. Sci. Conf. 31st. #1057.

Ehrenreich, A., Widdel, F., 1994. Anaerobic oxidation of ferrous iron by purple bacteria, a new type of phototrophic metabolism. Appl. Environ. Microb. 60, 4517–4526.

Farquhar, J., Thiemens, M.H., Jackson, T., 1998. Atmosphere–surface interactions on Mars: $\Delta^{17}O$ measurements of carbonate from ALH 84001. Science 280, 1580–1582.

Fischer, W.R., Schwertmann, U., 1975. The formation of hematite from amorphous iron (III) hydroxide. Clays Clay Miner. 23, 33–37.

Forget, F., Pierrehumbert, R.T., 1997. Warming early Mars with carbon dioxide clouds that scatter infrared radiation. Science 278, 1273–1276.

Foose, M.P., McLelland, J.M., 1995. Proterozoic low-Ti iron oxide deposits in New York and New Jersey: relation to Fe-oxide (Cu–U–Au–rare earth element) deposits and tectonic implications. Geology 23, 665–668.

Frost, B.R., 1991. Introduction to oxygen fugacity and its petrologic importance. Rev. Mineral. 25, 1–9.

Frost, B.R., Ballhaus, C., 1998. Comment on "Constraints on the origin of the oxidation state of mantle overlying subduction zones: an example from Simcoes, Washington, USA" by A.D. Brandon, D.S. Draper. Geochim. Cosmochim. Acta 62, 329–331.

Fyfe, W.S., Price, N.J., Thompson, A.B., 1978. Fluids in the Earth's Crust. Elsevier, New York.

Gay-Lussac, M., 1823. Réflexions sur les volcans. Ann. Chem. Phys. Ser. II 22, 415–429.

Gilmore, M.S., Tanake, K.L., 2002. Crater counts of MOC images within the Mars exploration rover Sinus Meridiani (hematite site) landing ellipses. In: Proc. Lunar Planet. Sci. Conf. 33rd. #1881 (abstract).

Golombek, M., 16 colleagues, 2002. Downselection of landing sites for the Mars Exploration Rovers. In: Proc. Lunar Planet. Sci. Conf. 33rd. #1245 (abstract).

Greeley, R., 1987. Release of juvenile water on Mars: estimated amounts and timing associated with volcanism. Science 236, 1653–1654.

Hamade, T., Phoenix, V., Konhauser, K., 2000. Photochemical and biologically mediated precipitation of iron and silica. In: Goldschmidt 2000, International Conference for Geochemistry September 3–8, 2000, Oxford, England. Abstract.

Hartman, H., McKay, C.P., 1995. Oxygenic photosynthesis and the oxidation state of Mars. Planet. Space Sci. 43, 123–128.

Hartmann, W.K., Anguita, J., de La Casa, M.A., Berman, D.C., Ryan, E.V., 2001. Martian cratering 7: the role of impact gardening. Icarus 149, 37–53.

Heising, S., Richter, L., Ludwig, W., Schink, B., 1999. Chlorobium ferrooxidans sp. nov., a phototrophic green sulfur bacterium that oxidizes ferrous iron in a coculture with a 'Geospirillum' sp. strain. Arch. Microbiol. 172, 116–124.

Herd, C.D.K., Papike, J.J., 2000. Oxygen fugacity of the martian basalts from analysis of iron–titanium oxides: implications for mantle–crust interaction on Mars. Meteorit. Planet. Sci. 35 (Suppl.). A70.

Hippert, J., Lana, C., 1998. Aerial crystallization of hematite in impact bombs from the Araguainha astrobleme, Matto Gross, central Brazil. Meteorit. Planet. Sci. 33, 1303–1309.

Holland, H.D., 1984. The Chemical Evolution of the Atmosphere and Oceans. Princeton Univ. Press, Princeton.

Holland, H.D., 2002. Volcanic gases, black smokers, and the Great Oxidation Event. Geochim. Cosmochim. Acta 66, 3811–3826.

Huck, F.O., Jobson, D.J., Park, S.K., Wall, S.D., Arvidson, R.E., Patterson, W.R., Benton, W.D., 1977. Spectrophotometric and color estimates of the Viking lander sites. J. Geophys. Res. 82, 4401–4411.

Hund, F., 1981. Inorganic pigments: basis for colored, uncolored and transparent properties. Angew. Chem. Int. Edit. 20, 723–730.

Hunten, D.M., 1973. The escape of light gases from planetary atmospheres. J. Atmos. Sci. 30, 1481–1494.

Hynek, B.M., Phillips, R.J., 2001. Evidence for extensive denudation of the martian highlands. Geology 29, 407–410.

Hynek, B.M., Arvidson, R.E., Phillips, R.J., 2002. Geologic setting and origin of Terra Meridiani hematite deposit on Mars. J. Geophys. Res. 107, 18.1–18.14.

Jakosky, B.M., Shock, E.L., 1998. The biological potential of Mars, the early Earth, and Europa. J. Geophys. Res. 103, 19359–19364.

Johnston, J.H., Lewis, D.G., 1983. A detailed study of the transformation of ferrihydrite to hematite in an aqueous solution at 92 °C. Geochim. Cosmochim. Acta 47, 1823–1831.

Kasting, J.F., 1991. CO_2 condensation and the climate of early Mars. Icarus 94, 1–13.

Keith, T.E.C., 1984. Preliminary observations on fumarole distribution and alteration, Valley of 10,000 smokes, Alaska. US Geol. Surv. Circ. 939, 82–85.

Kelsey, C., Hartmann, W.K., Grier, J.A., Berman, D.C., 2000. Observations of a hematite-rich region within Sinus Meridiani. In: Proc. Lunar Planet. Sci. Conf. 31st. #1524 (abstract).

Kerker, M., Scheiner, P., Cooke, D.D., Kratohvil, J.P., 1979. Absorbance index and color of colloidal hematite. J. Colloid Interf. Sci. 71, 176–187.

Kirschvink, J.L., Kim, S., Weiss, B.P., Shannon, D.M., Kobayashi, A.K., 2002. Rock magnetic and ferromagnetic resonance tests of biogenic magnetite in ALH84001. In: Proc. Lunar. Planet. Sci. Conf. 33rd. #1991 (abstract).

Kolb, E.D., Caporoso, A.J., Laudise, R.A., 1973. Hydrothermal growth of hematite and magnetite. J. Crystal Growth 19, 242–246.

Kral, T.A., Brink, K.M., Miller, S.L., McKay, C.P., 1998. Hydrogen consumption by methanogens on the early Earth. Origins Life Evol. B. 28, 311–319.

Krasnopolsky, V.A., Feldman, P.D., 2001. Detection of molecular hydrogen in the atmosphere of Mars. Science 294, 1914–1917.

Kwak, T.A.P., Brown, W.M., Abeysinghe, P.B., Tan, T.H., 1986. Fe solubilities in very saline hydrothermal fluids: their relation to zoning in some ore deposits. Econ. Geol. 81, 447–465.

Langmuir, D., 1971. Particle size effect on the reaction goethite = hematite + water. Amer. J. Sci. 271, 147–156.

Lane, M.D., Morris, R.V., Christensen, P.R., 1999. The spectral behavior of hematite at visible/near infrared and midinfrared wavelengths. In: The Fifth International Conference on Mars. Lunar and Planetary Institute, Houston. (CD-ROM). Abstract # 6085. LPI Contribution No. 972.

Lane, M.D., Morris, R.V., Christensen, P.R., 2000. Sinus Meridiani shows spectral evidence for oriented hematite grains. In: Proc. Lunar Planet. Sci. Conf. 31st. #1140 (abstract).

Lane, M.D., Hartmann, W.K., Berman, D.C., 2001. Update on studies of the martian hematite-rich areas. In: Proc. Lunar Planet. Sci. Conf. 32nd. #1984.

Lane, M.D., Morris, R.V., Hartmann, W.K., Christensen, P.R., Mertzman, S.A., 2002a. Platy hematite and metamorphism on Mars. In: Proc. Lunar. Planet. Sci. Conf. 33rd. #2020 (abstract).

Lane, M.D., Morris, R.V., Mertzman, S.A., Christensen, P.R., 2002b. Evidence for platy hematite grains in Sinus Meridiani Mars. J. Geophys. Res. 107, 9.1–9.15.

Laudise, R.A., 1970. The Growth of Single Crystals. Prentice–Hall, Englewood Cliffs, NJ.

Levin, G.V., 2002. Iron(VI) seems an unlikely explanation for Viking labeled release results. Icarus 159, 266–267.

Liu, S.C., Donahue, T.M., 1976. The regulation of hydrogen and oxygen escape from Mars. Icarus 28, 231–246.

Lyons, J.I., 1988. Volcanogenic iron oxide deposits, Cerro de Mercado and vicinity, Durango, Mexico. Econ. Geol. 83, 1886–1906.

Malin, M.C., Edgett, K.S., 2000. Sedimentary rocks of early Mars. Science 290, 1927–1937.

Malin, M.C., Edgett, K.S., 2001. The Mars Global Surveyor Mars Orbiter Camera: interplanetary cruise through primary mission. J. Geophys. Res. 106, 23429–23570.

Martin, R.F., Piwinskii, A.J., 1969. Experimental data bearing on the movement of iron in an aqueous vapor. Econ. Geol. 64, 798–803.

McElroy, M.B., 1972. Mars: an evolving atmosphere. Science 175, 443–445.

McKay, D.S., Gibson, E.K., Thomas-Keprta, K.L., Vali, H., Romanek, C.S., Clemett, S.J., Chiller, X.D.F., Maechling, C.R., Zare, R.N., 1996. Search for past life on Mars: possible relic biogenic activity in martian meteorite ALH84001. Science 273, 924–930.

McSween, H.Y., 1994. What we have learned about Mars from SNC meteorites? Meteoritics 29, 757–779.

Melnik, Y.P., 1982. Precambrian Banded Iron Formations. Elsevier, New York.

Mellon, M.T., Jakosky, B.M., 1995. The distribution and behavior of martian ground ice during past and present epochs. J. Geophys. Res. 100, 11781–11799.

Millero, F.J., Sotolongo, S., Izaguirre, M., 1987. The oxidation kinetics of Fe(II) in seawater. Geochim. Cosmochim. Acta 51, 793–801.

Minitti, M.E., Lane, M.D., Bishop, J.L., 2002a. Oxidized volcanic materials as a potential explanation for gray hematite regions on Mars. In: Proc. Lunar. Planet. Sci. Conf. 33rd. #1674 (abstract).

Minitti, M.E., Mustard, J.F., Rutherford, M.J., 2002b. Effects of glass content and oxidation on the spectra of SNC-like basalts: applications to Mars remote sensing. J. Geophys. Res. 107, 6.1–6.16.

Morris, R.V., Lauer Jr., H.V., Lawson, C.A., Gibson Jr., E.K., Nace, G.A., Stewart, C., 1985. Spectral and other physicochemical properties of sub-micron powders of hematite (α-Fe_2O_3), maghemite (γ-Fe_2O_3), magnetite (Fe_3O_4), goethite (α-FeOOH), and lepidocrocite (γ-FeOOH). J. Geophys. Res. 90, 3126–3144.

Morris, R.V., Agresti, D.G., Lauer Jr., H.V., Newcomb, J.A., Shelfer, T.D., Murali, A.V., 1989. Evidence for pigmentary hematite on Mars based on optical magnetic and Mossbauer studies of superparamagnetic (nanocrystalline) hematite. J. Geophys. Res. 94, 2760–2778.

Morris, R.V., Golden, D.C., Bell III, J.F., 1997. Low-temperature reflectivity spectra of red hematite and the color of Mars. J. Geophys. Res. 102, 9125–9133.

Morris, R.V., Golden, D.C., Bell III, J.F., Lauer Jr., H.V., 1995. Hematite, pyroxene, and phyllosilicates on Mars: implications from oxidized impact melt rocks from Manicouagan Crater, Quebec, Canada. J. Geophys. Res. 100, 5319–5328.

Morris, R.V., Golden, D.C., Bell III, J.F., Shelfer, T.D., Scheinost, A.C., Hinman, N.W., Furniss, G., Mertzman, S.A., Bishop, J.L., Ming, D.W., Allen, C.C., Britt, D.T., 2000. Mineralogy, composition, and alteration of Mars Pathfinder rocks and soils: evidence from multispectral, elemental, and magnetic data on terrestrial analogue, SNC meteorite, and Pathfinder samples. J. Geophys. Res. 105, 1757–1817.

Morris, R.V., Lauer Jr., H.V., 1981. Stability of goethite (a-FeOOH) and lepidocrocite (g-FeOOH) to dehydration by UV radiation: implications for their occurrence on the martian surface. J. Geophys. Res. 86, 10893–10899.

Noreen, E.D., Chapman, M.G., Tanaka, K.L., 2001. Possible formation processes for martian crystalline hematite. In: Field Trip and Workshop on the Martian Highlands and Mojave Desert Analogs, October 20–27, 2001, Las Vegas, Nevada, and Barstow, California. #4018 (abstract).

Nyström, J.O., Henríquez, F., 1994. Magmatic features of iron ores of the Kiruna type in Chile and Sweden: ore textures and magnetite geochemistry. Econ. Geol. 89, 820–839.

Oreskes, N., Rhodes, A.L., Rainville, K., Sheets, S., Espinoza, S., Zentilli, M., 1994. Origins of magnetite deposits at El Laco Chile: new evidence from field studies, fluid, inclusions, stable isotopes, and fission track analysis. Geol. Soc. Amer. Abstr. with Programs 26. A-379 (abstract).

Owen, T., 1992. The composition and early history of the atmosphere of Mars. In: Kieffer, H.H., Jackosky, B.M., Snyder, C.W., Matthews, M.S. (Eds.), Mars. Univ. of Arizona Press, Tucson, pp. 818–834.

Park, C.F., 1961. A magnetite "flow" in northern Chile. Econ. Geol. 56, 431–436.

Parkinson, I.J., Arculus, R.J., 1999. The redox state of subduction zones: insight from arc-peridotites. Chem. Geol. 160, 409–423.

Parkinson, W.D., 1983. Introduction to Geomagnetism. Elsevier, New York.

Parak, T., 1975. Kiruna type ores are not "intrusive-magmatic ores of the Kiruna type." Econ. Geol. 70, 1242–1248.

Perry Jr., E.C., Tan, F.C., Morey, G.B., 1973. Geology and stable isotope geochemistry of the Biwabik Iron Formation, northern Minnosota. Econ. Geol. 68, 1110–1125.

Phinney, W.C., Simonds, C.H., Cochran, A., McGee, P.E., 1978. West Clearwater, Quebec impact structure, Part II: petrology. In: Proc. Lunar Planet. Sci. Conf. 9th, pp. 2659–2693.

Pollack, J.B., Pitman, D., Khare, B., Sagan, C., 1970. Goethite on Mars: a laboratory study of physically and chemically bound water in ferric oxides. J. Geophys. Res. 75, 7480–7490.

Powell, C.M., Oliver, N.H.S., Zheng-Xiang, L., Martin, D.M., Ronaszeki, J., 1999. Synorogneic hydrothermal origin for giant Hamersley iron oxide. Geology 27, 175–178.

Reyes, D.P., Christensen, P.R., 1993. Evidence for ultramafic lavas on Syrtis Major. In: Lunar and Planetary Inst., Mars: Past, Present, and Future. Results from the MSATT Program, Part 1, pp. 44–45.

Roy, R.F., Beck, A.E., Touloukian, Y.S., 1989. Thermophysical properties of rocks. In: Ho, C.Y., Touloukian, Y.S., Judd, W.R., Roy, R.F. (Eds.), Physical Properties of Rocks and Minerals. Hemisphere, New York, pp. 409–502.

Russell, M.J., Hall, A.J., 1999. On the inevitable emergence of life on Mars. In: Hiscox, J.A. (Ed.), The Search for Life on Mars, Proceedings of the First UK Conference. British Interplanetary Society, pp. 26–36.

Schaefer, M.W., 1996. Are there abiotically-precipitated iron-formations on Mars? In: Dyar, M.D., McCammon, C., Schaefer, M.W. (Eds.), Mineral Spectroscopy: A Tribute to Roger G. Burns. In: Geochemical Society Special Publications Series, Vol. V.

Schubert, G., Solomon, S.C., Turcotte, D.L., Drake, M.J., Sleep, N.H., 1992. Origin and thermal evolution of Mars. In: Kieffer, H.H., et al. (Eds.), Mars. Univ. of Arizona Press, Tucson, pp. 147–183.

Schubert, G., Turcotte, D.L., Olson, P., 2001. Mantle Convection in the Earth and Planets. Cambridge Univ. Press, New York.

Schmalz, R.A., 1959. A note on the system Fe_2O_3–H_2O. J. Geophys. Res. 64, 575–579.

Seeger, C.M., Marikos, M.A., Nuelle, L.M., 1989. The Pilot Knob hematite deposit. In: Brown, V.M., Kisvarsanyi, E., Hagni, R. (Eds.), "Olympic Dam-type" Deposits and Geology of Middle Proterozoic Rocks in the St. Francois Mountains Terrane, Missouri: Guidebook, Vol. 4. Society of Economic Geologists, Fort Collins, pp. 55–68.

Sharp, R.P., 1973. Mars: fretted and chaotic terrain. J. Geophys. Res. 78, 4073–4083.

Sheets, S.A., Oreskes, N., Rhodes, A.L., Bodnar, R.J., Szabo, C., 1997. Fluid inclusion evidence for a hydrothermal origin for magnetite–apatite mineralization El Laco, Chile. In: GSA Annual Meeting Abstracts. #50418 (abstract).

Sherman, D.M., Waite, T.D., 1985. Electronic spectra of Fe^{3+} oxides and oxide hydroxides in the near IR and near UV. Am. Mineral. 70, 1262–1269.

Siever, R., 1992. The silica cycle in the Precambrian. Geochim. Cosmochim. Acta 56, 3265–3272.

Sleep, N.H., Zahnle, K., 1998. Refugia from asteroid impacts on early Mars and the early Earth. J. Geophys. Res. 103, 28529–28544.

Smith, D.E., 22 colleagues, 2001. Mars Orbiter Laser Altimeter (MOLA): experiment summary after the first year of global mapping of Mars. J. Geophys. Res. 106, 23689–23722.

Sugimoto, T., Waki, S., Itoh, H., Muramatsu, A., 1996. Preparation of monodisperse platelet-type hematite particles from a highly condensed β-FeOOH suspension. Colloids Surfaces A 109, 155–165.

Tanaka, K.L., Chapman, M., Johnson, J., Titus, T., 2000. Examination of igneous alternatives to martian hematite using terrestrial analogs. GSA Abstracts with Programs 32 (7). #52142 (abstract).

Taylor, D., Dalstra, H.J., Harding, A.E., Broadbent, G.C., Barley, M.E., 2001. Genesis of high-grade hematite orebodies of the Hamersley Province, Western Australia. Econ. Geol. 96, 837–873.

Thorkelson, D.J., Mortensen, J.K., Davidson, G.J., Creaser, R.A., Perez, W.A., Abbott, J.G., 2001. Early Mesoproterozoic intrusive breccias in Yukon, Canada: the role of hydrothermal systems in reconstructions of North America and Australia. Precambrian Res. 111, 31–55.

Torres-Ruiz, J., 1983. Genesis and evolution of the Marquesado and adjacent iron ore deposits, Granada, Spain. Econ. Geol. 78, 1657–1673.

Trendall, A.F., Blockley, J.G., 1970. The iron formations of the Precambrian Hamersley Group, Western Australia; with special reference to the associated crocidolite. Western Australia Geol. Surv. Bull. 119.

Tsang, W., Hampson, R.F., 1986. Chemical kinetic data base for combustion chemistry. Part 1. Methane and related compounds. J. Phys. Chem. Ref. Data 15, 1087–1279.

Tsapin, A.I., Goldfeld, M.G., McDonald, G.D., Nealson, K.H., Moskovitz, B., Solheid, P., Kemner, K.M., Kelly, S.D., Orlandini, K.A., 2000. Iron(VI): hypothetical candidate for the martian oxidant. Icarus 147, 68–78.

Tsapin, A., Goldfeld, M., Nealson, K., 2002. Viking's experiments and hypothesis that Fe(VI) is a possible candidate as a martian oxidant. Icarus 159, 268.

Vorobyeva, K.A., Melnik, Y.P., 1977. An experimental study of the system of Fe_2O_3–H_2O at $T = 100$–$200\,°C$ and P up to 9 kilobars. Geochem. Int. 8, 108–115.

Wadhwa, M., 2001. Redox state of Mars' upper mantle and crust from Eu anomalies in shergottite pyroxenes. Science 291, 1527–1530.

Walker, J.C.G., 1977. Evolution of the Atmosphere. Macmillan, New York.

Walker, J.C.G., 1978. Oxygen and hydrogen in the primitive atmosphere. Pure Appl. Geophys. 116, 222–231.

Walker, J.C.G., 1987. Was the Archean biosphere upside-down? Nature 329, 710–712.

Wänke, H., Dreibus, G., 1994. Chemistry and accretion history of Mars. Philos. Trans. R. Soc. London A 349, 285–293.

Wänke, H., Brückner, J., Dreibus, G., Ryabchikov, I., 2001. Chemical composition of rocks and soils at the Pathfinder site. Space Sci. Rev. 96, 317–330.

Wefers, K., 1966. On the system Fe_2O_3–H_2O. Part 1. Ber. Deutsch. Keram. Ges. 43, 677–702.

Widdel, F., Schnell, S., Heising, S., Ehrenreich, A., Assmus, B., Schink, B., 1993. Ferrous iron oxidation by anoxygenic phototrophic bacteria. Nature 362, 834–836.

Williams, H., Turner, F.T., Gilbert, C.M., 1954. Petrography: An Introduction to the Study of Rocks in Thin Section. Freeman, San Francisco.

Wollast, R., 1974. The silica problem. In: Goldberg, E.D. (Ed.). In: The Sea, Vol. 5. Wiley, New York, pp. 359–392.

Wood, B.J., 1991. Oxygen barometry of spinel peridotites. Rev. Mineral. 25, 417–431.

Wyatt, M.B., McSween, H.Y., 2002. Spectral evidence for weathered basalt as an alternative to andesite in the northern lowlands of Mars. Nature 417, 263–266.

Young, E.D., Galy, A., Nagahara, H., 2002. Kinetic and equilibrium mass-dependent isotope fractionation laws in nature and their geochemical and cosmochemical significance. Geochim. Cosmochim. Acta 66, 1095–1104.

Zies, E.G., 1929. Fumerolic incrustations and their bearing on ore deposition. Natl. Geogr. Soc. Contr., Tech. Papers 1, 1–61.